**Operational and Investment Solutions for Dynamic Line Switching and Rating in Electrical Grid**

by

Masood Jabarnejad

A dissertation proposal submitted to the Graduate Faculty of
Auburn University
in partial fulfillment of the
requirements for the Degree of
Doctor of Philosophy

Auburn, Alabama
August 1, 2015

Keywords: Seasonal Transmission Switching, Dynamic Thermal Rating, Decomposition, Benders Decomposition, Mixed Integer Programming, Power Generation Dispatch and Economics



Approved by

Jorge Valenzuela, Chair, Full Professor of Industrial and Systems Engineering
Jianhui Wang, Affiliated Professor of Industrial and Systems Engineering
Chase Murray, Assistant Professor of Industrial and Systems Engineering
Fadel Megahed, Assistant Professor of Industrial and Systems Engineering

Acknowledgments

I would like to express my special thanks to my advisor, Dr. Jorge Valenzuela for his endless support and mentorship. Without him, I would not be able to complete this dissertation. I appreciate the fact that he never gave up on me and his door was always open to me.

I would like to thank the faculties in my dissertation committee, Dr. Jianhui Wang, Dr. Chase Murray, and Dr. Fadel Megahed. Dr. Wang financially supported me through a funded research program for one and half year. Dr. Murray has always helped me out with my academic and professional questions since the day I started my Ph.D. program in Auburn. I also appreciate constructive feedbacks from Dr. Megahed regarding my research. I am thankful to all my committee members for their continuous support and friendship.

Last but not least, I want to thank my parents, my brother, and my sisters, for their eternal love for me and for their endless support. Without their love and attention, I would not be the person I am now and I would not be able to accomplish my graduate studies. Undoubtedly, I am successful in my life because of them and I proudly dedicate my Ph.D. dissertation to my family.

Table of Contents

List of Figures

List of Tables

# Introduction

The electricity generation industry is one of the most expensive infrastructures and one of the major sources of greenhouse gas emissions among other industries. A great deal of short-term and long-term decisions have been made to accelerate the transition of the electricity infrastructure toward a more cost-efficient and sustainable industry. This trend leads to future dependencies on both tradi- tional and renewable sources of energy that are naturally disseminated in different geographies and are often far from major energy consumption centers. How to effi- ciently transmit the diverse and disseminated sources of energy is one of the greatest management challenges in the future smart grids. In this dissertation two new trans- mission management approaches are developed that can result in the cost-efficient and environmentally-friendly utilization of the dispersed and diverse sources of en- ergy. The developed approaches are summarized in the following.

1. The transmission line network is usually considered a static structure when determining the optimal economic dispatch of power generators. The economics of the power dispatch can be improved by switching transmission lines into/out of service. The hourly-based economic transmission switching (TS) has been introduced in literature. In practice, the TS operation itself is a system disruptive action. In other words, frequently switching lines into or out of service can create undesirable effects in the security and reliability of power systems and may require new investments in the automation and control systems. In this PhD dissertation, the economic seasonal TS is proposed as an alternative transmission management approach to the hourly-based TS. In the proposed

seasonal TS, transmission switching occurs once at the beginning of a time period (season) and then the transmission topology remains unchanged during that period. The proposed seasonal transmission switching model is a large-scale mixed integer programming problem. The objective of the optimization model is to minimize the total energy generation cost over the season subject to loads and reliability requirements. The proposed model is demonstrated on typical power systems where the solutions are analyzed and potential cost savings in each case are reported. Our approach provides reduction in the operational costs for electric power companies and in the case of broad implementation it can reduce the price of electricity and save billions of dollars for the country.

2. The electric transmission network is constrained to thermal limits. Normally thermal ratings for lines are calculated based on conservative weather conditions which are called static ratings. Static ratings do not reflect the true transmission capability of lines and lead to less utilization of transmission elements. Dynamic thermal ratings (DTR), on the other hand, measure the thermal capacity of lines based on real time factors. It has been shown that the usage of the DTR in transmission systems allows more power flow through lines without sacrificing the reliability of the system. The improvement in utilization of existing transmission capacity can significantly reduce the electricity generation cost. Currently, most of transmission systems apply static ratings. Not to mention that benefiting from dynamic ratings requires investments on the DTR equipment. In this PhD dissertation, we also propose to integrate the dynamic rating system with transmission switching to further improve the economics and reliability of power systems and reduce emissions. Seasonal transmission switching requires minor investment costs and therefore those minor investments can be

neglected. However, utilizing dynamic ratings needs investments in new equipment. We model the investments in the dynamic rating system as a mixed integer linear program (MIP) where the transmission switching is allowed.

The remainder of this dissertation is organized as follows. Chapter 1 reviews the related work on transmission switching. Then the first proposed transmission management approach (seasonal TS) is described in detail. To solve the problem in reasonable time, a decomposition method is also developed in Chapter 1. Chapter 2 is devoted to the second proposed transmission management approach (integration of DTR with TS). In addition, an accelerated Benders decomposition is used for solving the model. Finally, Chapter 3 explores the effects of the proposed transmission management approaches on the emission reduction.

# Chapter 1

## A Decomposition Approach for Solving Seasonal Transmission Switching

### 1.1 Abstract

Economic transmission switching has been proposed as a new control paradigm to improve the economics of electric power systems. In practice, the transmission switching operation itself is a disruptive action to the system. Frequently switching lines into or out of service can create undesirable effects on the security and reliability of power systems and may require new investments in the automation and control systems. In this chapter, we formulate an economic seasonal transmission switching model where transmission switching occurs once at the beginning of a time period (season) and then the transmission topology remains unchanged during that period. The proposed seasonal transmission switching model is a large-scale mixed integer programming problem. The objective of the optimization model is to minimize the total energy generation cost over the season subject to loads and N-1 reliability requirements. We develop a novel decomposition method that decomposes the seasonal problem into one-hour problems which are then solved efficiently. We demonstrate our model and the decomposition approach on the 14-bus, 39-bus, and 118-bus power systems and show potential cost savings in each case.

**keywords:** seasonal transmission switching, decomposition, mixed integer programming, power generation dispatch and economics.

### Notations

Indices

$k$ Transmission lines

| | |
|---|---|
| $n$ | Generators |
| $u$ | Buses |
| $u_k$ | Origin bus for line $k$ |
| $v_k$ | Destination bus for line $k$ |
| $h$ | Hours |
| $b$ | Bins |
| $r$ | Contingency scenarios |

Sets

| | |
|---|---|
| $\Phi_u^-$ | Set of lines consuming power from bus $u$ |
| $\Phi_u^+$ | Set of lines injecting power to bus $u$ |
| $\Omega^{\mathbf{t}}$ | Set of in-service lines in transmission topology $\mathbf{t}$ |
| $\eta_u$ | Set of generators at bus $u$ |
| $\Upsilon$ | Set of buses with load |

Parameters

| | |
|---|---|
| $K$ | Number of transmission lines |
| $N$ | Number of generators |
| $U$ | Number of buses |
| $H$ | Number of hours |
| $B$ | Number of bins |
| $C_n$ | Operation cost of generator $n$ |
| $L_{uh}$ | Net load at bus $u$ at hour $h$ |

| | |
|---|---|
| $L'_{ub}$ | Representative load at bus $u$ in bin $b$ |
| $\widehat{L}_u$ | Peak load at bus $u$ in the planning season |
| $W_b$ | Number of load vectors in bin $b$ |
| $Y_k$ | Electrical susceptance of transmission line $k$ |
| $G_n^{\min}$, $G_n^{\max}$ | Min and max capacity of generator $n$ |
| $\theta_u^{\min}$, $\theta_u^{\max}$ | Min and max voltage angle at bus $u$ |
| $F_k^{\max}$ | Thermal Capacity of transmission line $k$ |
| $R_{kr}$ | State of line $k$ under scenario $r$ |
| $R'_{nr}$ | State of generator $n$ under scenario $r$ |
| $M_k$ | A sufficiently large number |
| $GC(\mathbf{t}, \mathbf{L})$ | Optimal generation cost under topology $\mathbf{t}$ at load vector $\mathbf{L}$ |

Variables

| | |
|---|---|
| $g_{nh}^r$ | Power generated by generator $n$ at hour $h$ under contingency scenario $r$ |
| $\theta_{uh}^r$ | Voltage angle at bus $u$ at hour $h$ under contingency scenario $r$ |
| $f_{kh}^r$ | Real Power flow transmitted by line $k$ at hour $h$ under contingency scenario $r$ |
| $x_u$ | Load variable for bus $u$ |
| $s$ | Objective function in the load lower-bound and load upper-bound problems |
| $z_k$ | Binary decision variable representing switching state of line $k$ (0 out of service, 1 in service) |
| $\mathbf{t}$ | Transmission topology ($\mathbf{t} = [z_1\ z_2\ \ldots\ z_K]$) |

## 1.2 Introduction

The transmission line network is usually considered a static structure when determining the optimal economic dispatch of power generators. However, it has been pointed out in [1] that switching transmission lines into/out of service has multiple benefits. The hourly-based optimal transmission switching (TS) problem was first introduced in [2]. It is modeled as a mixed integer program (MIP) based on the traditional DC optimal power flow (DCOPF) problem. The objective of the optimization model is to minimize the energy generation cost for one hour subject to supplying the load at that hour. The optimal TS problem was extended in [3] to include N-1 reliability requirements. Constraining the transmission switching to N-1 requirements ensures that the line on and off plan meets the NERC's single contingency reliability standard for power systems. A transmission switching model that includes unit commitment and N-1 constraints has been proposed in [4]. All of these studies have reported noticeable savings in power generation costs when using transmission switching.

Different aspects of the optimal TS problem have been reported in the literature [5–11]. A just-in-time concept has been added to the optimal TS problem in [5] to improve the efficiency of a power system by removing inefficient lines from service and only using those lines in unusual situations. The effects of transmission switching on electricity markets were investigated in [6]. The study showed that transmission switching may result in considerable variability in nodal prices, generator payments, and load payments. The authors concluded that the transmission topology planning should be controlled and managed by unbiased and independent agencies with no interest in the financial outcomes of the switching decisions. In [7], the authors developed a disjunctive programming model to enhance the static security of transmission switching operations. Transmission switching has also been applied in capacity expansion planning ( [8, 9]) and in security constrained unit commitment ( [10, 11]).

The formulated MIP for the hourly-based optimal TS is difficult to solve ( [2, 4, 12]). In [12] the authors show that the symmetry, the presence of more than one transmission line with the same impedance, thermal rating, and terminal buses, can adversely affect the computational requirement for solving the optimal TS problem. They introduce symmetry-breaking constraints and branching methods to deal with the symmetry in lines. To solve the optimal TS problem much faster, some heuristics have been proposed. A heuristic method has been reported in [13]. The method is based on a line-ranking parameter calculated using primal and dual solutions of the DCOPF problem. The line-ranking is used to detect lines that carry power flows from buses with high marginal cost to buses with low marginal cost. The detected lines are switched out of service. In [14] four transmission switching criteria are introduced to detect the switchable set of candidate lines. Another heuristic has been developed in [15]. The method uses two prescreening strategies to reduce the number of to-be-examined transmission lines for the optimal TS problem.

The economic transmission switching studies in [2–6] consider hourly TS for reducing costs. However, TS operation itself is a disruptive action and frequently switching lines into or out of service can create undesirable effects on the security and reliability of power systems [7]. In this chapter, we formulate an economic seasonal transmission switching (STS) model where the economic TS operation occurs once at the beginning of a time period (e.g. season) and then the transmission topology remains unchanged during that period (Figure 1). The objective of our STS model is to minimize the total generation cost over the season subject to loads and N-1 reliability requirements. We want to emphasize that the season can be defined to be a week, a month, or any other desired time period. It should be mentioned that periodic switching of transmission lines has been used for maintenance ( [16, 17]), and also for making trade-offs between protecting against potential contingencies in

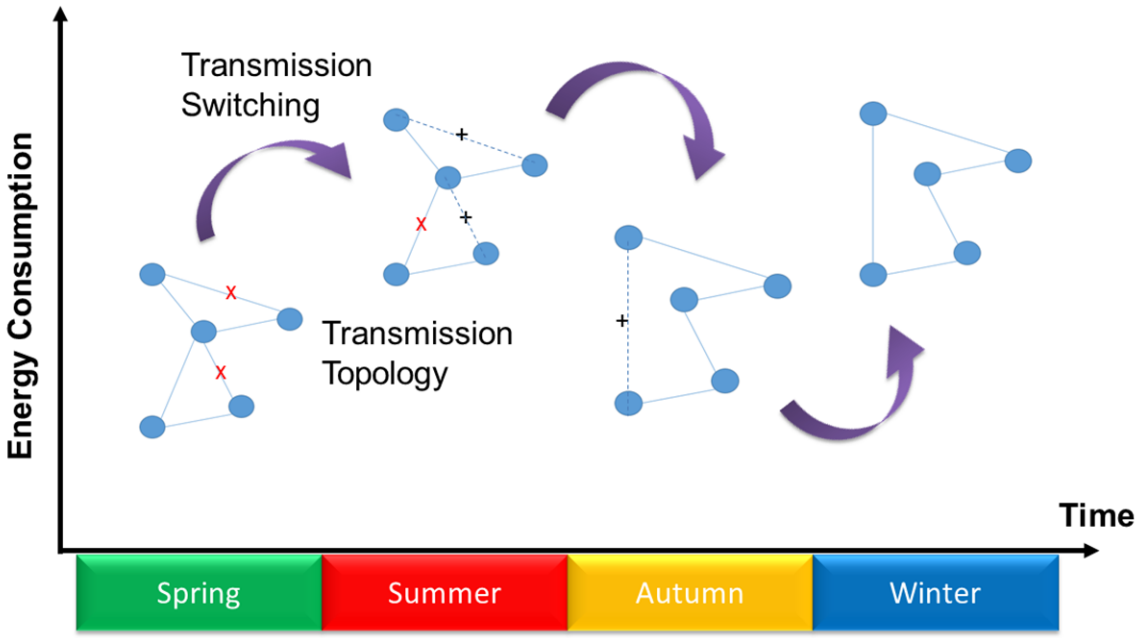


Figure 1: Seasonal Transmission Switching

winter versus avoiding potential overloads in summer [1]. Our seasonal TS focuses on the economics of switching for cost reductions. The contributions of this chapter are summarized as follows (1) The proposed STS model is unique in terms of considering the economic switching action once in a multiple time period which is studied for the first time in this chapter. (2) The STS model is very large in size compared to earlier TS models. The load lower-bound and upper-bound approaches, proposed in this chapter, significantly reduce the time required for solving the STS problem. (3) The decomposition approach introduced in this chapter is a novel method that enables breaking the seasonal problem into one-hour problems which can be solved in a reasonable time.

The rest of this chapter is organized as follows. Section 1.3 describes the STS model. To solve the STS model efficiently, a decomposition approach is developed in Section 1.4. Sections 1.5, 1.6, and 1.7 are devoted to conduct experiments of the STS model and the proposed decomposition approach on the 14-bus, 39-bus, and 118-bus

power systems. Section 1.8 analyzes the saving differences between the hourly and the seasonal TS. Section 1.9 gives the conclusions.

### 1.3 Seasonal Transmission Switching Model

The optimal TS problem in [2] is modeled as a mixed integer linear program where the transmission topology is assumed to be flexible. In this section, we model the economic seasonal transmission switching (STS) problem as a mixed integer linear program where the transmission topology can change only once in a multiple time period. Our model also includes the N-1 reliability requirements as in [18] and the variability of loads throughout the season. Since our model is for the mid-term seasonal planning purposes, we ignore the temporal constraints for the units such as ramping limits. The STS model is described by equations (1a) to (1g).

$$\text{Min} \sum_{h} \sum_{n} C_n g^0_{nh} \tag{1a}$$

Subject to

$$\sum_{n \in \eta_u} g^r_{nh} + \sum_{k \in \Phi^+_u} f^r_{kh} - \sum_{k \in \Phi^-_u} f^r_{kh} = L_{uh} \quad \forall\, u, r, h \tag{1b}$$

$$f^r_{kh} - R_{kr} Y_k (\theta^r_{u_k h} - \theta^r_{v_k h}) + (1 - z_k) M_k \geq 0 \quad \forall k, r, h \tag{1c}$$

$$f^r_{kh} - R_{kr} Y_k (\theta^r_{u_k h} - \theta^r_{v_k h}) - (1 - z_k) M_k \leq 0 \quad \forall k, r, h \tag{1d}$$

$$-F^{\max}_k R_{kr} z_k \leq f^r_{kh} \leq F^{\max}_k R_{kr} z_k \quad \forall k, r, h \tag{1e}$$

$$G^{\min}_n R'_{nr} \leq g^r_{nh} \leq G^{\max}_n R'_{nr} \quad \forall\, n, r, h \tag{1f}$$

$$\theta^{\min}_u \leq \theta^r_{uh} \leq \theta^{\max}_u \quad \forall\, u, r, h \tag{1g}$$

The objective function (1a) minimizes total electricity generation costs over the planning season when the system is operating without any contingency. Meeting all loads over the planning season is satisfied by constraints (1b). In the power balance constraints (1b), a net load $L_{uh}$ (i.e. the forcasted load minus the forecasted wind) at each hour is considered. The physical relations between voltage angles of connected buses and the power flow in connecting lines are represented by constraints (1c) and (1d). In constraints (1c) and (1d) the state of binary variables $z_k$ denotes that throughout the season line $k$ is either in service ($z_k = 1$) or switched out of service ($z_k = 0$). The $M_k$ is the disjunctive parameter. By setting the value of $M_k$ to be sufficiently large, the inequality constraints (1c) and (1d) will be redundant when the corresponding line is switched out of service. Efficiently tuning the disjunctive parameter $M_k$ is discussed in [19]. In this chapter, we use a fixed value of $|Y_k(\theta_u^{\max} - \theta_u^{\min})|$ for $M_k$ which was also used in [2]. Transmission thermal limits are enforced by constraints (1e), generators' capacity by (1f), and voltage angle limits by (1g). The left and right hand sides of constraints (1e) are multiplied by binary variables $z_k$ to ensure there is no power flow in lines that are out of service. The binary parameters $R_{kr}$ and $R'_{nr}$ are used in the model to include the N-1 contingency scenarios such as

$$R_{kr} = \left\{ \begin{array}{ll} 0 & \text{if } r = k \\ 1 & \text{otherwise} \end{array} \right\} \quad \forall\, k, r \tag{2a}$$

$$R'_{nr} = \left\{ \begin{array}{ll} 0 & \text{if } r = K + n \\ 1 & \text{otherwise} \end{array} \right\} \quad \forall\, n, r \tag{2b}$$

A value of $R_{kr} = 0$ means that line $k$ is under contingency and therefore it is not working. Similarly, a value of $R'_{nr} = 0$ means generator $n$ is not working. The non-contingency scenario (i.e. the normal operation without any contingency) is represented by constraints (1b)–(1g) with $r = 0$ to ensure that the system is feasible

(reliable) at every hour when there is no contingency. The N-1 contingency scenarios are represented by constraints (1b)–(1g) with $1 \leq r \leq K + N$.

### 1.4 A Decomposition Approach

The hourly-based TS problem is an NP-Hard problem [6]. The STS problem (1) is much larger than the hourly TS problem because it includes multiple time periods and N-1 reliability constraints. Directly solving the STS problem using CPLEX is difficult for small power systems and impossible for larger systems. To overcome this challenge we develop a decomposition approach. First, a few definitions are introduced and two properties of the STS problem are explored and proved. Then the decomposition approach is described in detail.

Given a load vector $\mathbf{L}_h$ at hour $h$, its total load is defined as the sum of its bus loads which is equal to $\sum_u L_{uh}$. The load vectors in a season are sorted with respect to their total loads in descending order. Therefore, in the set of sorted load vectors, the load vector with sort index 1 has the highest total load, the load vector with sort index 2 has the second highest total load, and so on. By the sort index of a load vector we mean the position of that load vector in the set of sorted load vectors, and not the hour that the load vector is forecasted. The sorted load vectors are grouped into $B$ bins. If bin $b$ is not the last bin (i.e. $1 \leq b \leq B-1$), then that bin includes load vectors with sort indexes $1 + (b-1)\lfloor H/B \rfloor$ to $b\lfloor H/B \rfloor$. If bin $b$ is the last bin (i.e. $b = B$), then it includes load vectors with sort indexes $1 + (B-1)\lfloor H/B \rfloor$ to $H$. Grouped load vectors in bin $b$ are represented by the representative load vector $\mathbf{L}'_b$ which has the highest total load in bin $b$, that is $\mathbf{L}'_b = \arg\max_{\mathbf{L}_i \in \Lambda}(\sum_u L_{ui})$ and $\Lambda_b = \{\mathbf{L}_i | \mathbf{L}_i \text{ is in bin } b\}$. In our decomposition approach, the goal is to find a transmission topology that minimizes the cost for supplying the representative load vectors and ensures supplying other load vectors in the planning season. The number of grouped load vectors in a bin ($W_b$) is used as a weight to estimate the total

generation cost for that bin. The user of our model can change the number of bins ($B$) in the model and make a trade-off between the amount of achieved cost reduction and the amount of time it takes to solve the problem. For example if a user sets $B = H$, then the STS model will include all load vectors in the season and the decomposition approach will find the optimal solution with the lowest generation cost. But it will take the longest time to solve the problem. Now consider the following problem.

$$\text{Min} \quad s \tag{3a}$$

Subject to

$$\frac{x_u}{\widehat{L}_u} \leq s \quad \forall\, u \in \Upsilon \tag{3b}$$

$$\sum_{n \in \eta_u} g_n^r + \sum_{k \in \Phi_u^+ \cap \Omega^{\mathbf{t}}} f_k^r - \sum_{k \in \Phi_u^- \cap \Omega^{\mathbf{t}}} f_k^r = x_u \quad \forall\, u, r \tag{3c}$$

$$f_k^r = R_{kr} Y_k \left(\theta_{u_k}^r - \theta_{v_k}^r\right) \quad \forall k \in \Omega^{\mathbf{t}}, r \tag{3d}$$

$$-F_k^{\max} \leq f_k^r \leq F_k^{\max} \quad \forall k \in \Omega^{\mathbf{t}}, r \tag{3e}$$

$$G_n^{\min} R'_{nr} \leq g_n^r \leq G_n^{\max} R'_{nr} \quad \forall\, n, r \tag{3f}$$

$$\theta_u^{\min} \leq \theta_u^r \leq \theta_u^{\max} \quad \forall\, u, r \tag{3g}$$

$$x_u \geq 0 \quad \forall\, u \in \Upsilon \quad \text{and} \quad x_u = 0 \quad \forall\, u \notin \Upsilon \tag{3h}$$

The problem (3) is a modified DCOPF problem in which the transmission network is fixed to the topology $\mathbf{t}$. As the problem (3) is for one hour, we dropped the hour index ($h$) from all variables and parameters. The problem (3) is a minimax problem where we want to minimize the maximum ratio of the bus load to the peak load at

all buses i.e. $\min \max_{u \in \Upsilon}(x_u/\widehat{L}_u)$. The value of the variable $s$ represents the largest ratio of the load variables to the peak loads. Constraints (3b) implement the minimax structure of the problem. The equations (3c) ensure that the net power balance at each bus meets the load variable $x$. The power flow equations, thermal ratings, generators' capacity, and voltage angle bounds are represented by constraints (3d)–(3g), respectively. The goal of the problem (3) is to find the lowest load vector $\mathbf{x}$ that can be supplied under the fixed topology $\mathbf{t}$. We call the problem (3) the load lower-bound (LLB) problem. The load upper-bound (LUB) problem is obtained from the LLB problem where we maximize the variable $s$ instead of minimizing it and we change the sign $\leq$ in constraints (3b) to $\geq$.

**Property 1.** *Let $\mathbf{x}^{LB}$ and $\mathbf{x}^{UB}$ denote optimal load solutions to the LLB and LUB problems, respectively. Then any load vector in the set $\chi = \{\mathbf{x} \mid x_u^{LB} \leq x_u \leq x_u^{UB}\ \forall x_u^{LB} \in \mathbf{x}^{LB}, x_u \in \mathbf{x}, x_u^{UB} \in \mathbf{x}^{UB}\}$ satisfies the constraints (3c)–(3h).*

*Proof.* Assume that $\varphi$ denotes the solution space for constraints (3c)–(3h). Because constraints (3c)–(3h) are linear, the $\varphi$ is a convex polyhedron. This means that the solutions inside or on the edge of $\varphi$ satisfy constraints (3c)–(3h). As constraints (3c)–(3h) in both LLB and LUB problems are the same, the load solutions $\mathbf{x}^{\mathrm{LB}}$ and $\mathbf{x}^{\mathrm{UB}}$ are inside or on the edge of $\varphi$. All load vectors in the set $\chi$ are between load solutions $\mathbf{x}^{\mathrm{LB}}$ and $\mathbf{x}^{\mathrm{UB}}$ and therefore inside or on the edge of the $\varphi$ which concludes that any $\mathbf{x} \in \chi$ satisfies constraints (3c)–(3h). □

Property 1 indicates that for checking the feasibility of a topology $\mathbf{t}$ in a season, it is enough to check the feasibility of $\mathbf{t}$ at load vectors $\mathbf{L}_h \notin \chi$. We call a transmission topology as global feasible if that topology satisfies constraints (1b)–(1g) for all hours $h = 1, \ldots, H$. Also we call a topology as global optimal at load vectors $\mathbf{L}_1, \mathbf{L}_2, \ldots, \mathbf{L}_i$ if that topology is the optimal solution to the problem (1) with load vectors $\mathbf{L}_1, \mathbf{L}_2, \ldots, \mathbf{L}_i$. Now assume that instead of solving the STS problem (1) with

all representative load vectors, we solve the problem with one particular load vector. The following property holds for the STS problem (1) with one-hour load.

**Property 2.** *Assume* $\mathbf{t}_i^*$ *and* $\mathbf{t}_j^*$ *are global feasible and optimal topologies at load vectors* $\mathbf{L}_i$ *and* $\mathbf{L}_j$*, respectively. Also assume that* $\mathbf{t}_{\{i,j\}}^*$ *is the global optimal topology at load vectors* $\mathbf{L}_i$ *and* $\mathbf{L}_j$*. Then the inequality* $GC(\mathbf{t}_j^*, \mathbf{L}_j) \leq GC(\mathbf{t}_{\{i,j\}}^*, \mathbf{L}_j) \leq GC(\mathbf{t}_i^*, \mathbf{L}_j)$ *holds. Note that* $GC(\mathbf{t}, \mathbf{L})$ *denotes the optimal objective function value (generations cost) under topology* $\mathbf{t}$ *at load vector* $\mathbf{L}$*.*

*Proof.* This property is proved by contradiction. Assume that the inequality $GC(\mathbf{t}_j^*, \mathbf{L}_j) \leq GC(\mathbf{t}_{\{i,j\}}^*, \mathbf{L}_j) \leq GC(\mathbf{t}_i^*, \mathbf{L}_j)$ does not hold. This means either $GC(\mathbf{t}_{\{i,j\}}^*, \mathbf{L}_j) < GC(\mathbf{t}_j^*, \mathbf{L}_j)$ or $GC(\mathbf{t}_{\{i,j\}}^*, \mathbf{L}_j) > GC(\mathbf{t}_i^*, \mathbf{L}_j)$ holds. The inequality $GC(\mathbf{t}_{\{i,j\}}^*, \mathbf{L}_j) < GC(\mathbf{t}_j^*, \mathbf{L}_j)$ is not satisfied as it violates the optimality of the topology $\mathbf{t}_j^*$ at load vector $\mathbf{L}_j$. On the other hand, the topology $\mathbf{t}_i^*$ is optimal at load vector $\mathbf{L}_i$ and its objective function value is the lowest satisfying $GC(\mathbf{t}_{\{i,j\}}^*, \mathbf{L}_i) > GC(\mathbf{t}_i^*, \mathbf{L}_i)$. By adding two inequalities $GC(\mathbf{t}_{\{i,j\}}^*, \mathbf{L}_j) > GC(\mathbf{t}_i^*, \mathbf{L}_j)$ and $GC(\mathbf{t}_{\{i,j\}}^*, \mathbf{L}_i) > GC(\mathbf{t}_i^*, \mathbf{L}_i)$ we have $GC(\mathbf{t}_{\{i,j\}}^*, \mathbf{L}_i) + GC(\mathbf{t}_{\{i,j\}}^*, \mathbf{L}_j) > GC(\mathbf{t}_i^*, \mathbf{L}_i) + GC(\mathbf{t}_i^*, \mathbf{L}_j)$. This means topology $\mathbf{t}_i^*$ is a better solution at load vectors $\mathbf{L}_i$ and $\mathbf{L}_j$ than topology $\mathbf{t}_{\{i,j\}}^*$ which violates the assumption that topology $\mathbf{t}_{\{i,j\}}^*$ is the global optimal at load vectors $\mathbf{L}_i$ and $\mathbf{L}_j$. □

Property 2 indicates that for finding the global optimal topology at load vectors $\mathbf{L}_i$ and $\mathbf{L}_j$ it is enough to enumerate the candidate topologies with generation costs in the range $[GC(\mathbf{t}_j^*, \mathbf{L}_j), GC(\mathbf{t}_i^*, \mathbf{L}_j)]$. This property is better illustrated in Figure 2. In Figure 2, the horizontal axis is for the representative load vectors and the vertical axis is for the corresponding electricity generation costs. The optimal topology for the load vector $\mathbf{L}_i$ is $\mathbf{t}_i^*$. The electricity generation cost for $\mathbf{t}_i^*$ at load vector $\mathbf{L}_j$ is lower than its cost at load vector $\mathbf{L}_i$. The optimal topology for load vector $\mathbf{L}_j$ is $\mathbf{t}_j^*$. At load vector $\mathbf{L}_j$, topologies $\mathbf{t}_a$ and $\mathbf{t}_b$ have lower electricity generation costs than $\mathbf{t}_i^*$ and higher electricity generation costs than $\mathbf{t}_j^*$. At load vectors $\mathbf{L}_j$, the electricity

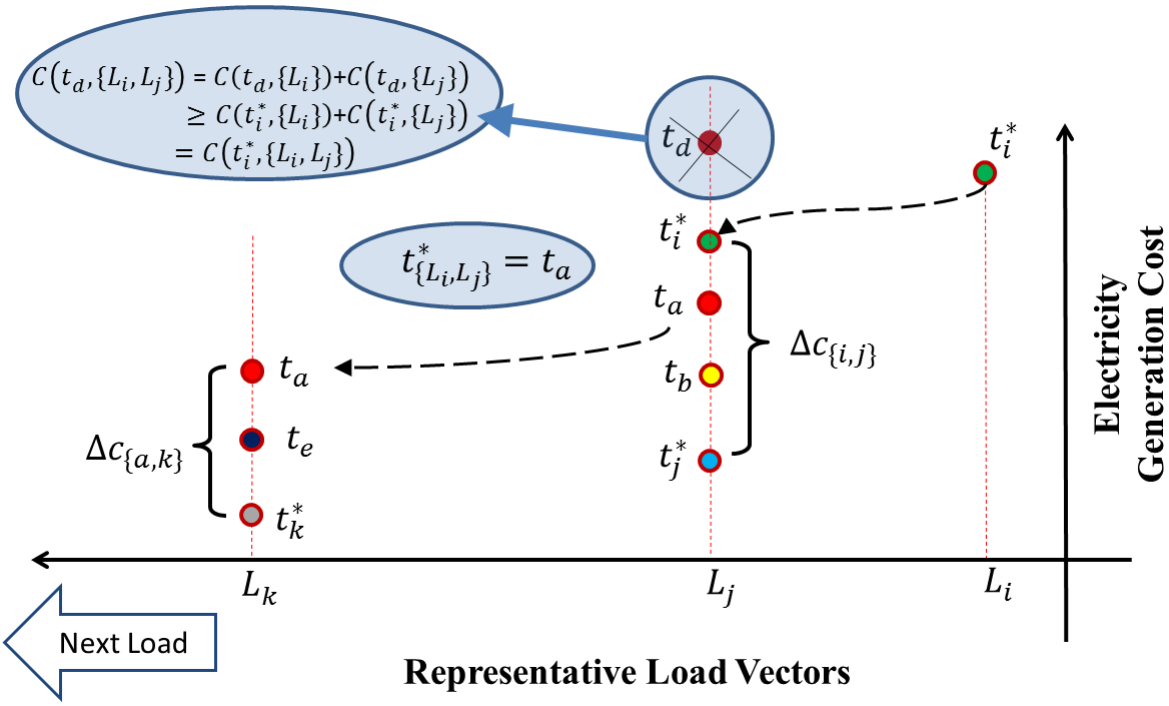


Figure 2: Searching the Global Optimal Topology (Property 2)

generation cost for the topology $\mathbf{t}_d$ is higher than the one for the topology $\mathbf{t}_i^*$. As it is shown in the figure, the cumulative cost for the $\mathbf{t}_d$ at load vectors $\mathbf{L}_i$ and $\mathbf{L}_j$ is higher than the one for the $\mathbf{t}_i^*$. However, the same conclusion cannot be reached for the topologies $\mathbf{t}_a$ and $\mathbf{t}_b$. Between candidate topologies $\mathbf{t}_i^*$, $\mathbf{t}_a$, $\mathbf{t}_b$, and $\mathbf{t}_j^*$, the topology $\mathbf{t}_a$ is assumed to have the lowest cumulative cost at load vectors $\mathbf{L}_i$ and $\mathbf{L}_j$. Therefore, $\mathbf{t}_a$ is the global optimal topology at load vectors $\mathbf{L}_i$ and $\mathbf{L}_j$ and is kept for the next iteration. At the next iteration, the cost of $\mathbf{t}_a$ is evaluated at third load vector ($\mathbf{L}_k$). To be able to find the global optimal topology at load vectors $\mathbf{L}_i$, $\mathbf{L}_j$, and $\mathbf{L}_k$, it is sufficient to compare the cumulative costs of candidate topologies $\mathbf{t}_a$, $\mathbf{t}_e$, and $\mathbf{t}_k^*$ and there is no need to consider topologies that have higher cost than $\mathbf{t}_a$ at load vector $\mathbf{L}_k$. This process can be continued for the next load vectors until all of them are enumerated.

Properties 1 and 2 are used to develop a decomposition algorithm. First the STS problem is decomposed into one-hour load problems. The algorithm solves the STS problem with load vector $\mathbf{L}_1$ and finds the optimal topology at $\mathbf{L}_1$. Based on Property 2, the algorithm moves to the STS problem with load vector $\mathbf{L}_2$ and finds the global optimal topology at $\mathbf{L}_1$ and $\mathbf{L}_2$. Then the algorithm moves to load vector $\mathbf{L}_3$ and finds the global optimal topology at $\mathbf{L}_1$, $\mathbf{L}_2$, and $\mathbf{L}_3$. The algorithm continues to iterate until all considered load vectors are enumerated. Property 1 is used at each iteration to efficiently check the global feasibility of candidate topologies.

The pseudocode of the proposed decomposition algorithm is provided in Figures 3 and 4. In the main code in steps 4 through 7, the lines are switched out of service one at a time and the feasibility and generation cost of the resulting transmission network is examined. Using the obtained information, a heuristic is used in steps 8 through 12 to construct an initial topology that is feasible and also results in less generation cost than the full topology without transmission switching. The constructed topology is denoted in the code as $\mathbf{t}$. In steps 13 through 15 the $\mathbf{t}$ is used to find the initial optimal topology at the representative load vector at first bin considering the N-1 constraints. First, the optimal topology $\mathbf{t}_1^*$ at the first representative load without considering N-1 constraints is found in step 13. In step 14, the candidate topologies with generation cost lower than or equal to the cost of $\mathbf{t}$ and higher than or equal to the cost of $\mathbf{t}_1^*$ are collected in the set $\omega$. The function "EnumTopols()" is used in step 15 to find the best topologies in $\omega$ and report as the initial global optimal topologies at the representative load vectors considering the N-1 constraints.

The function "EnumTopols()", defined in Figure 4 in steps 23 through 35, enumerates input topologies and finds the best one(s) in terms of global feasibility and least generation cost over all representative load vectors. The defined function requires a set of candidate topologies ($\omega$), a set of current global topologies ($\Gamma$) at

**/*** construction of an initial feasible topology ***/**

1) $\mathbf{L}'_1 \leftarrow$ representative load vector at first bin
2) $\mathbf{t}(0) \leftarrow [z_1^0\ z_2^0\ \ldots\ z_K^0]$ where $z_j^0 \leftarrow 1$ for all $j = 1, 2, \ldots, K$
3) $\Psi \leftarrow \emptyset$; $\omega \leftarrow \emptyset$; $\Gamma \leftarrow \emptyset$
4) for $k = 1$ to $K$ {
5) $\quad \mathbf{t}(k) \leftarrow [z_1^k\ z_2^k\ \ldots\ z_K^k]$ where $z_j^k \leftarrow 0$ if $j = k$ and
$\quad\quad z_j^k \leftarrow 1$ if $j \neq k$ for all $j = 1, 2, \ldots, K$
6) $\quad$ if $\mathbf{t}(k)$ is feasible in (1a)–(1g) /* Property 1 */
$\quad$ and if $GC(\mathbf{t}(k), \mathbf{L}'_1) < GC(\mathbf{t}(0), \mathbf{L}'_1)$ then $\Psi \leftarrow \Psi \cup \{k\}$
7) }
8) $\mathbf{t} \leftarrow [z_1\ z_2\ \ldots\ z_K]$ where $z_j \leftarrow 1$ for all $j = 1, 2, \ldots, K$
9) While $\Psi \neq \emptyset$ {
10) $\quad z_j \leftarrow 0$ where $GC(\mathbf{t}(j), \mathbf{L}'_1)$ is the smallest for all $k \in \Psi$
11) $\quad$ if $\mathbf{t}$ is infeasible in (1a)–(1g) then $z_j \leftarrow 1$ /* Property 1 */
12) $\quad \Psi \leftarrow \Psi \backslash \{j\}$ }

**/*** the initial optimal topology ***/**

13) $\mathbf{t}_1^* \leftarrow$ the optimal topology from solving (1a)–(1g) with $\mathbf{L}'_1$
and $r = 0$
14) $\omega \leftarrow$ candidate topologies with obj. fun. values in the range
$\quad [GC(\mathbf{t}_1^*, \mathbf{L}'_1),\ GC(\mathbf{t}, \mathbf{L}'_1)]$ /* Property 2 */
15) $(\Gamma, mincost) \leftarrow \text{EnumTopols}(\omega, \{\mathbf{t}\}, GC(\mathbf{t}, \mathbf{L}'_1))$

**/*** decomposition ***/**

16) for $b = 2$ to $B$ {
17) $\quad gtopol \leftarrow$ first element in $\Gamma$
18) $\quad \mathbf{t}_b^* \leftarrow$ the optimal topology from solving (1a)–(1g) with $\mathbf{L}'_b$
$\quad$ and $r = 0$
19) $\quad \omega \leftarrow$ candidate topologies with obj. fun. values in the range
$\quad [GC(\mathbf{t}_b^*, \mathbf{L}'_b),\ GC(gtopol, \mathbf{L}'_b)]$ /* Property 2 */
20) $\quad (\Gamma, mincost) \leftarrow \text{EnumTopols}(\omega, \Gamma, mincost)$
21) }
22) Return $\Gamma, mincost$

Figure 3: A Pseudocode for Proposed Decomposition Algorithm: Part I

```
    /*** function definition ***/
23) EnumTopols(ω, Γ, mincost) {
24)   gtopol ← first element in Γ
25)   Repeat    /* enumerate candidate topologies */
26)     topol ← first element in set ω
27)     if topol is feasible in (1a)–(1g)    /* Property 1 */
        then {
28)       cost ← Σ_{j=1}^{B} GC(topol, L'_j)
29)       if cost < mincost then { /* a better topology */
30)         mincost ← cost; gtopol ← topol; Γ ← {topol} }
31)       if cost = mincost then { /* multiple topologies */
32)         Γ ← Γ ∪ {topol} } }
33)     ω ← ω\{topol}
34)   Until ω = ∅
35)   Return Γ, mincost }
```

Figure 4: A Pseudocode for Proposed Decomposition Algorithm: Part II

representative load vectors, and their generation cost (*mincost*) as input parameters. It then checks the feasibility (step 27) and calculates the cumulative generation cost (step 28) for each topology in $\omega$. In steps 29 to 32, the global topologies at representative load vectors are compared with other topologies and updated if it is necessary. Also the topologies that have cumulative generation costs same as the global topologies at representative load vectors, are added to the set $\Gamma$. The set of global topologies at representative load vectors and the cost are reported in step 35. In the second part of the main code (steps 16 through 22), the decomposition approach is applied. In the loop in steps 16 through 21 the remaining representative load vectors are enumerated and their global optimal topologies are updated. In step 18, the optimal topology in the next representative load without considering N-1 constraints is found ($\mathbf{t}_b^*$). Then in step 19, the candidate topologies with generation cost

lower than or equal to the cost of current global optimal topology at representative load vectors and higher than or equal to the cost of $\mathbf{t}_b^*$ are collected in the set $\omega$. In step 20, the function "EnumTopols()" updates global optimal topologies at representative load vectors considering N-1 constraints. After all representative load vectors are considered, the final global optimal topologies at representative load vectors and total generation cost are reported in step 22. A lookup table is used to discard the already known infeasible topologies or the detected inferior topologies (in terms of total generation cost) from further reexaminations.

In the following sections, we test the seasonal transmission switching on the 14-bus, the 39-bus and the 118-bus cases from the IEEE reliability test system [20] and from [21], using the actual data from the Pennsylvania, New Jersey and Maryland Interconnection (PJM) [22]. We implement our developed decomposition algorithm using C programming language and we use the CPLEX Version 12.5 to collect candidate topologies and to solve the LPs and MIPs. All experiments are conducted on a computer with Intel(R) Celeron(R) CPU 1005M @ 1.90GHz and 4GB of RAM memory. Also the values of $\pm 0.6$ radians are considered for minimum/maximum voltage angles at all buses. The results are documented and discussed in the following sections.

### 1.5 Experimental Results on the 14-Bus System

The 14-bus power system [20] has 5 generators, 20 lines, and 11 loads, as shown in Figure 5. As the thermal capacities of transmission lines in the 14-bus system are not provided, we confined the maximum limit of power flow in every transmission line to 150MW. For each generator, the quadratic cost function, taken from Matpower [23], is replaced with one straight-line segment and the slope of the line is considered as the linearized cost coefficient for that generator. The 14-bus system is summarized in Table 1. To generate the seasonal loads, first we normalize the hourly load data

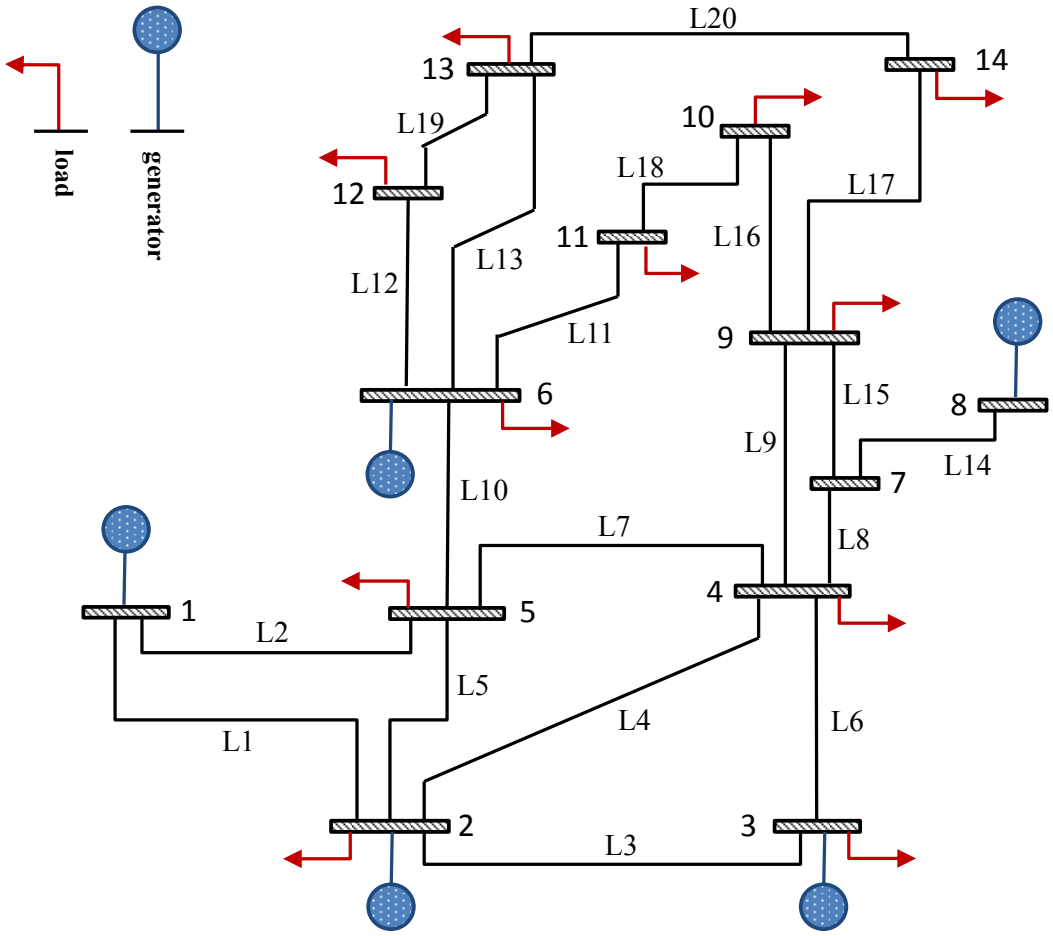


Figure 5: 14-bus power system

Table 1: 14-bus power system

| | | Capacity (MW) | | | Cost ($/MWh) | |
|---|---|---|---|---|---|---|
| | No. | Total | Min | Max | Min | Max |
| Generators | 5 | 772.4 | 100 | 332.4 | 34.3 | 55 |
| Transmission | 20 | 3000 | 150 | 150 | | |
| Load | 11 | 259 | 3.5 | 94.2 | | |

from [22] for the regions PJME, PJMW, and COMED and for the summer season (Jun01 - August31) of year 2012 which is $92 \times 24 = 2208$ hours of data for each region. We assume that, in the 14-bus system, the normalized load profile for buses 1 through 3 are the same with the normalized load profile for region PJME, for buses 4 through

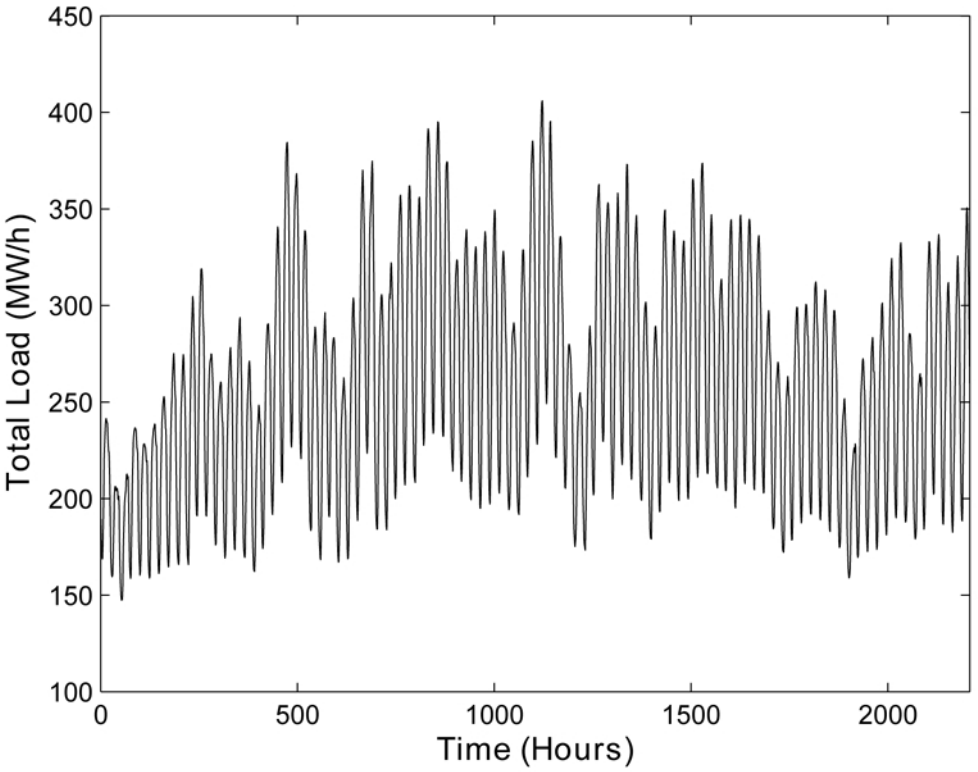


Figure 6: Total load in different hours of summer

6 the same with region PJMW, and for buses 7 through 14 the same with region COMED. The normalized load data in each region is multiplied by 1.6 times the corresponding system load at the 14-bus system to generate different loads at every hour. The 1.6 times the load at the 14-bus system represents the extreme power consumption in a typical hot summer. The generated seasonal load profile is depicted in Figure 6. We limit the maximum number of switchable line candidates to 1 and 2 respectively, and compare it with the case where no limit on the maximum number of switchable lines exists. Then we analyze the resulting impacts of the switching on the total generation cost and reliability requirements in the season.

### 1.5.1 Switching one line out of service

The transmission lines in the 14-bus system are switched out of service one at a time and the reduction or increase in costs are calculated. In the calculation of costs, the 2208 hours of load data is used. The results are summarized in Table 2 where the rows are sorted in ascending order of total cost in the season. The results show that switching one of the lines 3, 4, 5, 8, 9, 15, 16, or 17 out of service can decrease total generation costs. Switching line 4 out of service results in the lowest generation cost of $20,061,606, which is $194,752 or 0.96% saving. Switching line 3 or 5 out of service also results in considerable savings of 0.69% and 0.95% respectively. Switching any of lines 12, 18, and 19 out of service has the least impact on generation costs in the considered season. The worst impact on costs occurs when line 1 or 2 is removed from service, which results in 4.45% increase in costs. The power system without one of the lines 1, 2, 4, 5, 7, 8, 9, 10, 13, or 15 still remains N-1 reliable. Switching the line 4 out of service noticeably decreases the cost and preserves the N-1 reliability requirement.

### 1.5.2 Switching two lines out of service

Experiments with two lines out of service are conducted. There are 190 pair-wise combinations of the 20 lines in the 14-bus system. The N-1 reliability status is preserved in only 39 of the 190 pairs with two lines out of service. For those 39 pairs of lines with N-1 status, the percentages of cost savings are summarized in Table 3. In this table, L4 means line 4 is out of service, L5 means line 5 is out of service and so on. The values in Table 3 indicate the percentages of change in the generation cost if the corresponding lines in the very top and right are switched together. The highest saving, 2.83%, results from switching lines 4 and 5 out of service. When compared to seasonal generation cost with full topology operation, this is a $572,395 reduction in the cost. The second highest saving occurs when lines 5 and 15 are removed from

Table 2: Experiments With One Line Out of Service

| Switched Line | From Bus | To Bus | Total Cost in Season ($) | Savings (%) | N-1 Status |
|---|---|---|---|---|---|
| No Switch | – | – | 20,256,358 | – | Yes |
| Line 4 | 2 | 4 | 20,061,606 | 0.96 | Yes |
| Line 5 | 2 | 5 | 20,064,381 | 0.95 | Yes |
| Line 3 | 2 | 3 | 20,115,945 | 0.69 | No |
| Line 15 | 7 | 9 | 20,241,621 | 0.07 | Yes |
| Line 8 | 4 | 7 | 20,244,374 | 0.06 | Yes |
| Line 9 | 4 | 9 | 20,250,958 | 0.03 | Yes |
| Line 16 | 9 | 10 | 20,252,124 | 0.02 | No |
| Line 17 | 9 | 14 | 20,251,330 | 0.02 | No |
| Line 12 | 6 | 12 | 20,256,809 | 0 | No |
| Line 18 | 10 | 11 | 20,257,179 | 0 | No |
| Line 19 | 12 | 13 | 20,256,435 | 0 | No |
| Line 6 | 3 | 4 | 20,258,863 | -0.01 | No |
| Line 11 | 6 | 11 | 20,259,147 | -0.01 | No |
| Line 13 | 6 | 13 | 20,258,998 | -0.01 | Yes |
| Line 14 | 7 | 8 | 20,259,175 | -0.01 | No |
| Line 20 | 13 | 14 | 20,258,263 | -0.01 | No |
| Line 10 | 5 | 6 | 20,295,424 | -0.19 | Yes |
| Line 7 | 4 | 5 | 20,479,764 | -1.1 | Yes |
| Line 1 | 1 | 2 | 21,158,137 | -4.45 | Yes |
| Line 2 | 1 | 5 | 21,158,137 | -4.45 | Yes |

the service which results in 1.05% or $212,939 saving. The worst case occurs when one of lines 1 or 2 is switched along with any of lines 4, 5, 7, 8, 9, 10, 13, or 15 where it results in 4.45% increase in the generation cost.

Table 3: Savings (%) With Two Lines Out of Service

| | | | | | | | | | |
|---|---|---|---|---|---|---|---|---|---|
| L4 | | | | | | | | | |
| 2.83 | L5 | | | | | | | | |
| 0.99 | 1.05 | L15 | | | | | | | |
| 0.99 | 1.04 | INF* | L8 | | | | | | |
| 0.97 | 0.99 | INF* | 0.19 | L9 | | | | | |
| 0.95 | 0.93 | 0.06 | 0.05 | 0.01 | L13 | | | | |
| 0.86 | 0.67 | INF* | -0.25 | INF* | -0.19 | L10 | | | |
| INF* | -0.47 | -0.79 | -0.89 | -1.00 | -1.18 | -2.59 | L7 | | |
| -4.45 | -4.45 | -4.45 | -4.45 | -4.45 | -4.45 | -4.45 | -4.45 | L1 | |
| -4.45 | -4.45 | -4.45 | -4.45 | -4.45 | -4.45 | -4.45 | -4.45 | INF* | L2 |

* The INF means the resulting topology is infeasible.

### 1.5.3 Finding the optimal seasonal switching solution

In the third case, we do not limit the number of lines that can be switched out of service. In other words, any number of lines can be removed from service. The bin number is set to 100 and the representative load vectors are calculated in the same way explained in Section 1.4. After running the decomposition algorithm using the representative loads, it finds that the global optimal topology at representative load vectors is to switch lines 4, 5, and 15 out of service. The total generation cost of the found solution in the whole season with 2208 hours of loads is \$19,682,878, while if no-switching is allowed, the generation cost increases to \$20,256,358. The implementation of this solution gives a 2.83% reduction in cost (\$573,480 saving). The seasonal saving is consistent with the findings of experiments with one line and two lines out of service. The STS problem is solved by the decomposition algorithm with $B = 2208$ (i.e. with all 2208 load vectors) to validate the found optimal solution with $B = 100$ (i.e. with 100 representative load vectors). The solution with $B = 2208$ is the same with the findings of the model with $B = 100$. The decomposition algorithm

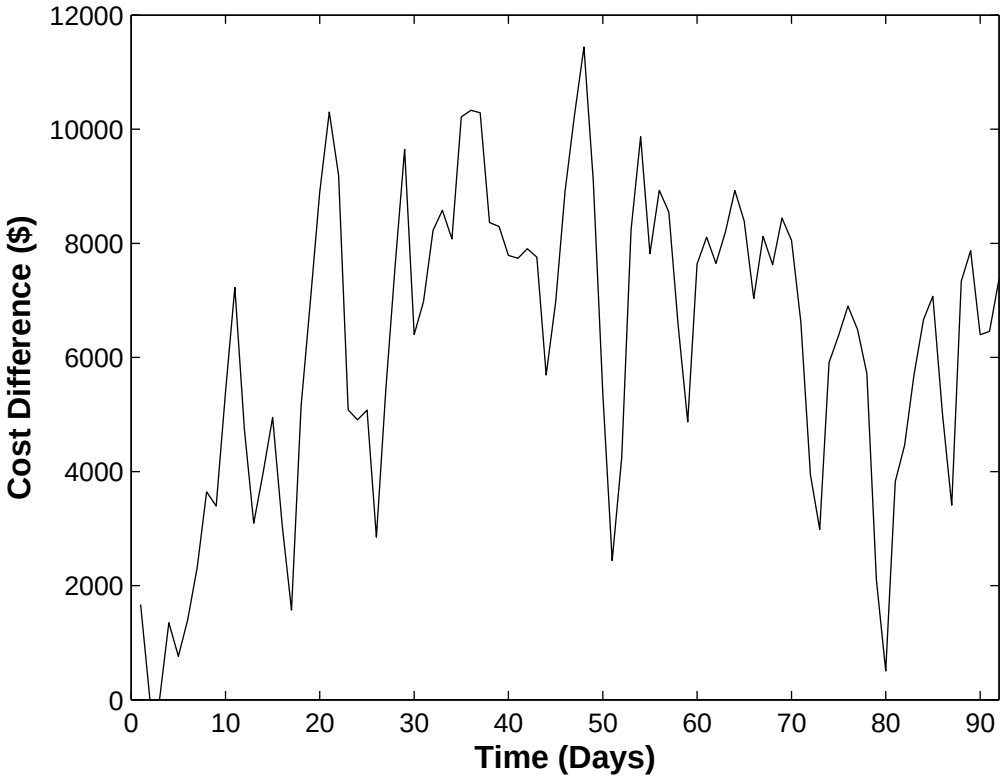


Figure 7: Generation cost difference between the full topology and the switched topology in different days

solves the problem with $B = 100$ in one and a half minutes and the problem with $B = 2208$ in 3 hours and 58 minutes. Hence, modeling the problem with representative loads reduces the computational time significantly and offers the same quality solution at the same time. We also applied CPLEX on the same problem with 2208 hours of loads. After 6 hours of running time, CPLEX could not find a transmission switching solution.

The differences in generation costs between the global optimal topology at representative load vectors and the full topology are depicted in Figures 7 and 8 on the daily basis and the total load basis, respectively. Figure 7 shows that the highest cost saving occurs during day 48 which corresponds to July 18. The results in Figure 7 are fairly consistent with the data in Figure 6, in which the severe peak-load hours are

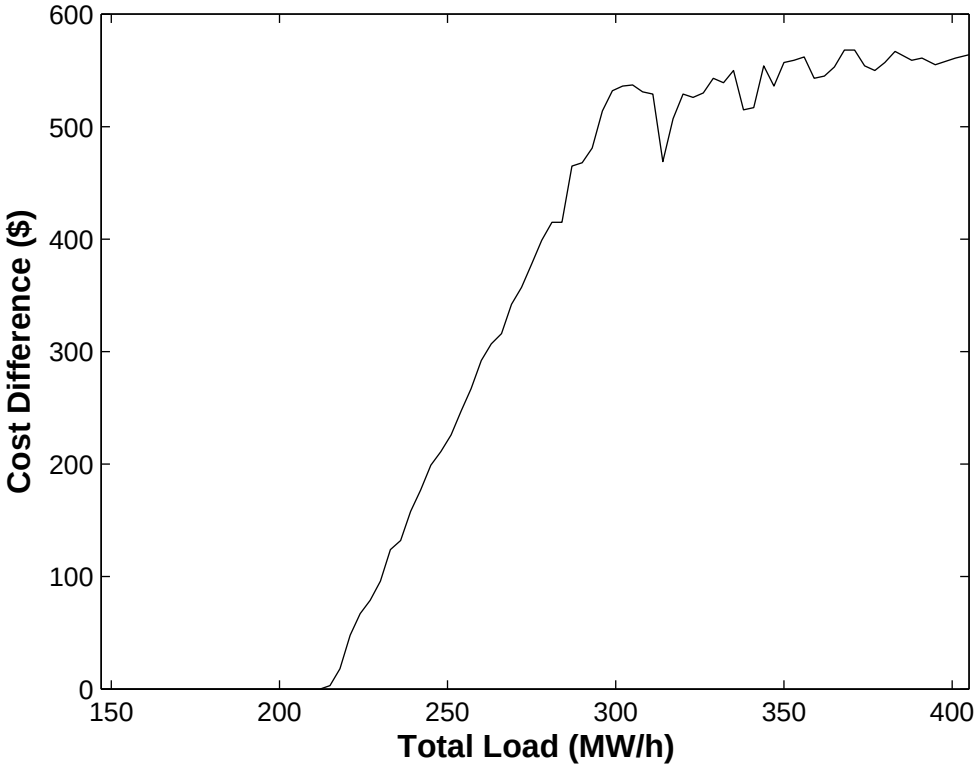


Figure 8: Generation cost difference between the full topology and the switched topology in different total loads

experienced in month of July. The relationship between peak-load times and saving amounts are better shown in Figure 8, in which the total loads for different hours are sorted from the lowest to the highest. As this figure indicates, there are positive cost differences at total loads 214MW/h to 406MW/h meaning that switching lines 4, 5, and 15 results in less generation cost at those total load levels. Nevertheless, switching the mentioned lines has no economic benefit at total loads 147MW/h to 213MW/h. The switching practice cumulatively outperforms the non-switching practice for the season because the generation costs are lower for higher total loads.

### 1.6 Experimental Results on the 39-Bus System

The 39-bus power system is a generally representative network of the New England 345KV system [21] and the data for this power system is taken from MatPower [23].

Table 4: 39-bus power system

| | | Capacity (MW) | | | Cost ($/MWh) | |
|---|---|---|---|---|---|---|
| | No. | Total | Min | Max | Min | Max |
| Generators | 10 | 7367 | 508 | 1100 | 5.38 | 22.05 |
| Transmission | 46 | 33530 | 250 | 1800 | | |
| Load | 21 | 6254.23 | 6.5 | 1104 | | |

The system is comprised of 10 generators, 46 lines, and 21 loads and is summarized in Table 4. Generation quadratic costs are linearized in the same way explained in previous experiments. After initial examinations, it is noticed that the 39-bus system is not N-1 reliable when the system load is considered. However, the system is reliable to single contingencies when 0.72 times of the system load or less is applied. Hence, for this power system a time period with moderate loads is considered to preserve N-1 reliability requirements. To generate the seasonal loads, first we normalize the hourly load data from [22] for the regions DOM, FE, and DEOK and for the time period from October 1 to December 31 of year 2012. We assume that the normalized load profile for buses 1 through 13 are the same with the normalized load profile for region DOM, for buses 14 through 26 the same with region FE, and for buses 27 through 39 the same with region DEOK. The normalized load data is multiplied by the corresponding system load at the 39-bus system to generate seasonal load data. Again for efficiency, we bin 2208 hours of loads into 100 representative load vectors in the same way explained before. We also decrease the power flow limit of the line (2-25) from 500MW to 250MW to create congestion.

We assume all lines can be switched and the optimization results show that removing lines 4, 10, and 13 from service and keeping the others in service is the optimal network configuration. The total generation cost of the found solution in the entire season is $48,233,701. If no transmission line is switched, the total generation

Table 5: IEEE 118-bus system

| | | Capacity (MW) | | | Cost ($/MWh) | |
|---|---|---|---|---|---|---|
| | No. | Total | Min | Max | Min | Max |
| Generators | 19 | 5859 | 100 | 805 | 0.1897 | 10 |
| Transmission | 186 | 49720 | 220 | 1100 | | |
| Load | 99 | 4519 | 2 | 440 | | |

cost is $49,301,768. This optimal network configuration for the 39-bus system saves $1,068,067 in 3 months while respecting N-1 requirements. This saving is 2.17% of total generation costs. The decomposition algorithm solves this problem in less than 7 minutes. The optimality of the found solution is validated by solving the problem by the decomposition algorithm with $B = 2208$. The topology solution obtained from the decomposition algorithm with $B = 2208$ is the same with the topology solution of the decomposition algorithm with $B = 100$. The decomposition algorithm solves the problem with $B = 2208$ in 6 hours and 22 minutes. Therefore, similar to the 14-bus system, binning the loads preserves the optimal solution and significantly reduces the computational time. The CPLEX gets out-of-memory when it is used to solve the STS problem on the 39-bus system with 2208 hours of loads.

### 1.7 Experimental Results on the 118-Bus System

Data for the IEEE 118-bus power system is downloaded from [20] where generators' capacity, generation costs, transmission network and line characteristics are taken from [24]. The 118-bus system is summarized in Table 12. We use the normalized load data used in the experiments on the 14-bus system. We assume that the normalized load profile for buses 1 through 40 are the same with the normalized load profile for region PJME, for buses 41 through 80 the same with region PJMW, and for buses 81 through 118 the same with region COMED. The normalized load data in each region is multiplied by the corresponding system load at the 118-bus system to

Table 6: Elements in the 118-bus System Removed From the N-1 Contingency List

| Generators | Transmission Lines |
|---|---|
| {13, 14, 15, 17} | Non-Radial Lines: {(77-82), (82-83), (85-88), (89-90), (89-92), (91-92)}<br>Radial Lines: {(8-9), (9-10), (12-117), (14-15), (16-17), (18-19), (29-31), (68-116), (71-73), (85-86), (86-87), (110-111), (110-112) } |

generate different loads at every hour. The radial transmission lines are not considered in the FERC's reliability standards [18]. Therefore, those elements are removed from the N-1 contingency list. The IEEE 118-bus system is not reliable to the single contingency scenarios if one of the generators or non-radial lines in Table 13 is lost. To make the system survive in N-1 scenarios, the generators and transmission lines listed in Table 13 are removed from the N-1 contingency list. The studies in [2, 25] show that limiting the number of out-of-service lines to a smaller number preserves the majority of the cost savings from transmission switching while it improves the computational efficiency. To speed up the process, the number of out-of-service transmission elements is limited to 5 lines and the number of bins is set to 10. We apply the decomposition algorithm on the system with modified N-1 contingency constraints. The decomposition algorithm finds the seasonal transmission solution to switch out of service the lines 77, 123, 132, 133, and 172. With those 5 lines switched out of service at the beginning of the season, total generation cost over 2208 hours of loads is \$1,426,286 where without switching any line, total generation cost is \$1,463,476. Therefore, \$37,190 is saved in whole season which is 2.54% reduction in total generation cost. The decomposition algorithm solves the problem in 5 hours and 52 minutes. The CPLEX gets out-of-memory when it is used to solve the STS problem on the 118-bus system with 2208 hours of loads.

## 1.8 Cost Savings

In this section, we compare the cost reductions of the hourly transmission switching (HTS) and the seasonal transmission switching (STS) on the 14-bus, 39-bus and 118-bus systems. In the 14-bus system with the HTS, the total generation cost in the season is \$19,681,464 which is a 2.83% reduction in the cost. The HTS saves \$1,414 (or 0.007%) more in the season when it is compared to the STS. In the 39-bus system, the total generation cost with the HTS is \$48,225,435 which is \$8,266 lower than the total generation cost with the STS. This is 0.017% improvement in the cost saving. Solving the TS problem on the 118-bus system with N-1 contingency scenarios is computationally difficult even for one hour load [3]. In the previous section we limited the number of out-of-service transmission elements to 5 lines and considered 10 representative load vectors for the 118-bus system to decrease the computational time of the STS. We consider the same limitation on maximum number of switchable lines (5 lines) and the same 10 representative load vectors for the HTS. The total generation cost in the considered 10 hours with the HTS is \$7,169 while with the STS the cost is \$7,414. With no transmission switching the cost increases to \$7,640 which results in 6.16% saving by HTS and 2.96% saving by STS, respectively. As the HTS has more flexibility in changing the transmission topology, when compared to the STS, in general it is expected that the HTS provides more cost reduction. More research is needed for a thorough evaluation of the cost reductions provided by HTS and STS methods.

## 1.9 Conclusions

Seasonal transmission switching can be an alternative approach to hourly-based transmission switching when new investments are undesirable and excessive transmission switching is avoided. We show that despite one-time switching at the beginning of the season, the seasonal transmission switching model can noticeably reduce generation

costs. A seasonal decision such as the STS problem probably would not have to be solved within a short time period which is required in the hourly TS problem. However, efficiently solving the STS problem is important because of two reasons: The STS model is itself a difficult problem to solve and efficiency becomes necessary when the size of the problem increases. Also, the long-term investment projects normally require simulation of various future scenarios where computational efficiency for such problems is required. The CPLEX could not find a cost-reducing solution to the 14-bus system after running for 6 hours. The CPLEX also gets out-of-memory when it is used to solve the STS problem on the 39-bus and 118-bus systems. The developed decomposition algorithm in this chapter significantly reduces the time required to solve the problem. The solution time is further decreased by binning thousands of load vectors into tractable number of representative load vectors. More research is needed to be conducted on power systems to investigate the sensitivity of good solutions to bin numbers and finding better criteria for effective data reduction for the STS problem. We used DC power flow and deterministic net-load profiles in our STS model. Future research should include the development of an AC-OPF STS model and the uncertainties especially in wind, which are two important extensions to our current deterministic model.

References

[1] K.W. Hedman, S.S. Oren, and R.P. O'Neill. A review of transmission switching and network topology optimization. In *Power and Energy Society General Meeting, 2011 IEEE*, pages 1 –7, july 2011.

[2] E.B. Fisher, R.P. O'Neill, and M.C. Ferris. Optimal transmission switching. *Power Systems, IEEE Transactions on*, 23(3):1346 –1355, aug. 2008.

[3] K.W. Hedman, R.P. O'Neill, E.B. Fisher, and S.S. Oren. Optimal transmission switching with contingency analysis. *Power Systems, IEEE Transactions on*, 24(3):1577 –1586, aug. 2009.

[4] K.W. Hedman, M.C. Ferris, R.P. O'Neill, E.B. Fisher, and S.S. Oren. Co-optimization of generation unit commitment and transmission switching with n-1 reliability. *Power Systems, IEEE Transactions on*, 25(2):1052 –1063, may 2010.

[5] K.W. Hedman, R.P. O'Neill, E.B. Fisher, and S.S. Oren. Smart flexible just-in-time transmission and flowgate bidding. *Power Systems, IEEE Transactions on*, 26(1):93 –102, feb. 2011.

[6] K.W. Hedman, R.P. O'Neill, E.B. Fisher, and S.S. Oren. Optimal transmission switching - sensitivity analysis and extensions. *Power Systems, IEEE Transactions on*, 23(3):1469 –1479, aug. 2008.

[7] Cong Liu, Jianhui Wang, and J. Ostrowski. Static switching security in multi-period transmission switching. *Power Systems, IEEE Transactions on*, 27(4):1850 –1858, nov. 2012.

[8] A. Khodaei, M. Shahidehpour, and S. Kamalinia. Transmission switching in expansion planning. *Power Systems, IEEE Transactions on*, 25(3):1722 –1733, aug. 2010.

[9] J.C. Villumsen and A.B. Philpott. Investment in electricity networks with transmission switching. *European Journal of Operational Research*, 222(2):377 – 385, 2012.

[10] A. Khodaei and M. Shahidehpour. Transmission switching in security-constrained unit commitment. *Power Systems, IEEE Transactions on*, 25(4):1937 –1945, nov. 2010.

[11] A. Khodaei and M. Shahidehpour. Security-constrained transmission switching with voltage constraints. *International Journal of Electrical Power & Energy Systems*, 35(1):74 – 82, 2012.

[12] J. Ostrowski, Jianhui Wang, and Cong Liu. Exploiting symmetry in transmission lines for transmission switching. *Power Systems, IEEE Transactions on*, 27(3):1708–1709, 2012.

[13] J.D. Fuller, R. Ramasra, and A. Cha. Fast heuristics for transmission-line switching. *Power Systems, IEEE Transactions on*, 27(3):1377 –1386, aug. 2012.

[14] P.A. Ruiz, J.M. Foster, A. Rudkevich, and M.C. Caramanis. Tractable transmission topology control using sensitivity analysis. *Power Systems, IEEE Transactions on*, 27(3):1550–1559, 2012.

[15] Cong Liu, Jianhui Wang, and J. Ostrowski. Heuristic prescreening switchable branches in optimal transmission switching. *Power Systems, IEEE Transactions on*, 27(4):2289 –2290, nov. 2012.

[16] M. K C Marwali and S. M. Shahidehpour. Long-term transmission and generation maintenance scheduling with network, fuel and emission constraints. *Power Systems, IEEE Transactions on*, 14(3):1160–1165, 1999.

[17] H. Pandzic, A.J. Conejo, I. Kuzle, and E. Caro. Yearly maintenance scheduling of transmission lines within a market environment. *Power Systems, IEEE Transactions on*, 27(1):407–415, 2012.

[18] Mandatory Reliability Standards for the Bulk Power System, U.S. Federal Energy Regulatory Commission. 2007, Order, 72 FR 16416.

[19] S. Binato, M. V F Pereira, and S. Granville. A new benders decomposition approach to solve power transmission network design problems. *Power Systems, IEEE Transactions on*, 16(2):235–240, May 2001.

[20] Power Systems Test Case Archive.

[21] G. W. Bills. On-line stability analysis study, October 12, 1970.

[22] PJM Hourly Load Data.

[23] R.J. Thomas R.D. Zimmerman, C.E. Murillo-Sanchez. Matpower: steady-state operations. Planning and analysis tools for power systems research and education. *IEEE Transactions on Power Systems*, 26:1219, 2011.

[24] S. Blumsack. Network topologies and transmission investment under electric-industry restructuring. PhD. dissertation, Dep. Eng. and Public Policy, Carnegie Mellon University, Pittsburgh, PA, 2006.

[25] C. Barrows and S. Blumsack. Transmission switching in the rts-96 test system. *Power Systems, IEEE Transactions on*, 27(2):1134 –1135, may 2012.

# Chapter 2

## Optimal Investment Plan for Dynamic Thermal Rating Using Benders Decomposition

### 2.1 Abstract

The dynamic thermal rating is a new technology that utilizes the capacity of power transmission lines based on the ambient factors and the line condition. It usually offers higher thermal capacity than the traditional static rating. We propose a multi-stage mixed integer programming model and find the optimal investment plan for the dynamic ratings using Benders Decomposition. The investment plan includes when and which line should be upgraded to dynamic rating and which line should be switched out of service. The problem is decomposed into a master problem and three sub-problems. The master problem explores the candidate lines for both the investment plan and the switching plan, throughout the planning horizon. The sub-problems evaluate the proposed plans in terms of unmet demand and generation cost. Generation and transmission contingencies are also included in the model. We use our model on Garver's system and a 118-bus power systems to demonstrate our solution approach. We conduct sensitivity analyses and study the uncertainty in real-time thermal ratings, loads, and the discounting rate. Our studies show that the utilization of the dynamic ratings and the practice of transmission switching are complementary and can reduce the cost on the 118-bus system up to 30%.

**keywords:** dynamic thermal rating, power generation dispatch and economics, transmission switching, mixed integer linear programming, benders decomposition.

### Notations

Indices

$k$ Transmission line.

| | |
|---|---|
| $n$ | Generator. |
| $b$ | Bus. |
| $a_k$ | Origin bus for line $k$. |
| $b_k$ | Destination bus for line $k$. |
| $t$ | Time period. |
| $l$ | Load block. |
| $r$ | Contingency ($r > 0$) or non-contingency ($r = 0$) scenario for power system elements. |

Sets

| | |
|---|---|
| $\Phi_b^-$ | Set of lines consuming power from bus $b$. |
| $\Phi_b^+$ | Set of lines injecting power to bus $b$. |
| $\Phi_b^\pm$ | Set of lines connected to bus $b$. |
| $\eta_b$ | Set of generators at bus $b$. |

Parameters

| | |
|---|---|
| $K$ | Number of transmission lines. |
| $N$ | Number of generators. |
| $B$ | Number of buses. |
| $T$ | Number of time periods. |
| $C_n^{\mathrm{g}}$ | Operational cost of generator $n$. |
| $C_k^{\mathrm{d}}$ | Investment cost for line $k$. |
| $I^{\mathrm{d}}$ | Capital dynamic rating investment. |

$i$ Discount rate.

$D_{tlb}$ Electricity demand at bus $b$ at time period $t$ at load block $l$.

$H_l$ Number of hours at load block $l$.

$E_k$ Electrical susceptance of transmission line $k$.

$G_n^{\min}$, $G_n^{\max}$ Min and max capacity for generator $n$.

$\Theta_k^{\max}$ Max phase angle difference between origin and destination buses for line $k$.

$F_k^{\mathrm{s}}$ Static thermal rating for transmission line $k$.

$\Delta F_k^{+}$ Minimum additional thermal rating for transmission line $k$.

$X_t^{\max}$ Max number of lines that can be invested at time period $t$.

$Z_{tl}^{\max}$ Max number of lines that can be out of service at time period $t$ at load block $l$.

$R_{rk}$ State of line $k$ under scenario $r$.

$R'_{rn}$ State of generator $n$ under scenario $r$.

Variables

$x_{tk}$ Investment state of line $k$ at time period $t$.

$z_{tlk}$ Switching state of line $k$ at time period $t$ at load block $l$.

$g_{tlrn}$ Power generated by generator $n$ under scenario $r$ at time period $t$ at load block $l$.

$\theta_{tlrb}$ Phase angle at bus $b$ under scenario $r$ at time period $t$ at load block $l$.

$f_{tlrk}$ Real power flow transmitted by line $k$ under scenario $r$ at time period $t$ at load block $l$.

$P$ Objective function of the master problem.

$s^{+}_{tlrb}, s^{-}_{tlrb}$ Energy shortage and excess at bus $b$ under scenario $r$ at time period $t$ at load block $l$.

$y_{tlrk}$ Logical variable for line $k$ under scenario $r$ at time period $t$ at load block $l$.

## 2.2 Introduction

The electric transmission network is a complex infrastructure and constrained to thermal limits that should not be exceeded. Normally thermal limits for lines are determined by static ratings which are calculated based on conservative weather conditions [1]. In the static rating model, the worst-case weather conditions are considered (a low conductor emissivity, a low wind speed, and the highest expected ambient temperature). This results in underestimating the line potential in power transfer during climatic conditions that are far from the worst-case. Therefore, the static rating model does not reflect the true transmission capability of lines and leads to less utilization of transmission elements [2]. The dynamic thermal rating (DTR), on the other hand, calculates the thermal capacity of lines based on the real-time line condition and surrounding ambient factors. Considering the real time ambient conditions results in better utilization of the transmission elements during the times in which the weather conditions match the long term averages.

The thermal rating of overhead lines is governed by a series of factors including the conductor size and its resistance, the current flowing in the conductor, and the ambient weather conditions [3–5]. Under steady-state conditions, the heat balance of a conductor is described in equations (4). In these equations, the $q_c$ denotes the convected-heat loss due to the wind speed and its direction, $q_r$ is the radiated-heat loss, $I$ is the conductor current, $R(T_c)$ is the AC resistance of the conductor in

temperature $T_c$, and $q_s$ is the amount of heat gained from the solar radiation and the ambient temperature.

$$q_c + q_r = I^2 R(T_c) + q_s \quad \Rightarrow \quad I = \sqrt{\frac{q_c + q_r - q_s}{R(T_c)}} \tag{4}$$

The thermal rating of a transmission line can be calculated and predicted using equations (4). Three widely used methods for calculating overhead line capacity are published by the Institute of Electrical and Electronics Engineers (IEEE) [5], the International Electrochemical Commission (IEC) [6], and the Council on Large Electric Systems (CIGRE) [7]. In [8] it has been shown that the usage of the DTR in transmission systems allows more power flow through lines without sacrificing the reliability of the system. The improvement in utilization of existing transmission capacity can significantly reduce the electricity generation cost [8].

Transmission switching (TS) is proposed as another approach to improve the economy of the electric power generation and dispatch [9–11]. In the TS approach the detected lines are temporarily switched out of service to increase the power flow from buses with low marginal cost to buses with high marginal cost. Using optimal transmission switching for the cost reduction was first introduced in [9]. The optimal TS problem is extended in [10] to include N-1 reliability requirements. Constraining the transmission switching to N-1 requirements ensures that the line on and off plan meets the demand requirements when any of the generation units or transmission lines is subject to the single contingency. A transmission switching model that includes unit commitment and N-1 constraints has been proposed in [11]. All these studies have reported noticeable savings in power generation costs when using transmission switching. Transmission switching is also used in transmission expansion problem [12, 13]. Although hourly transmission switching shows great potential

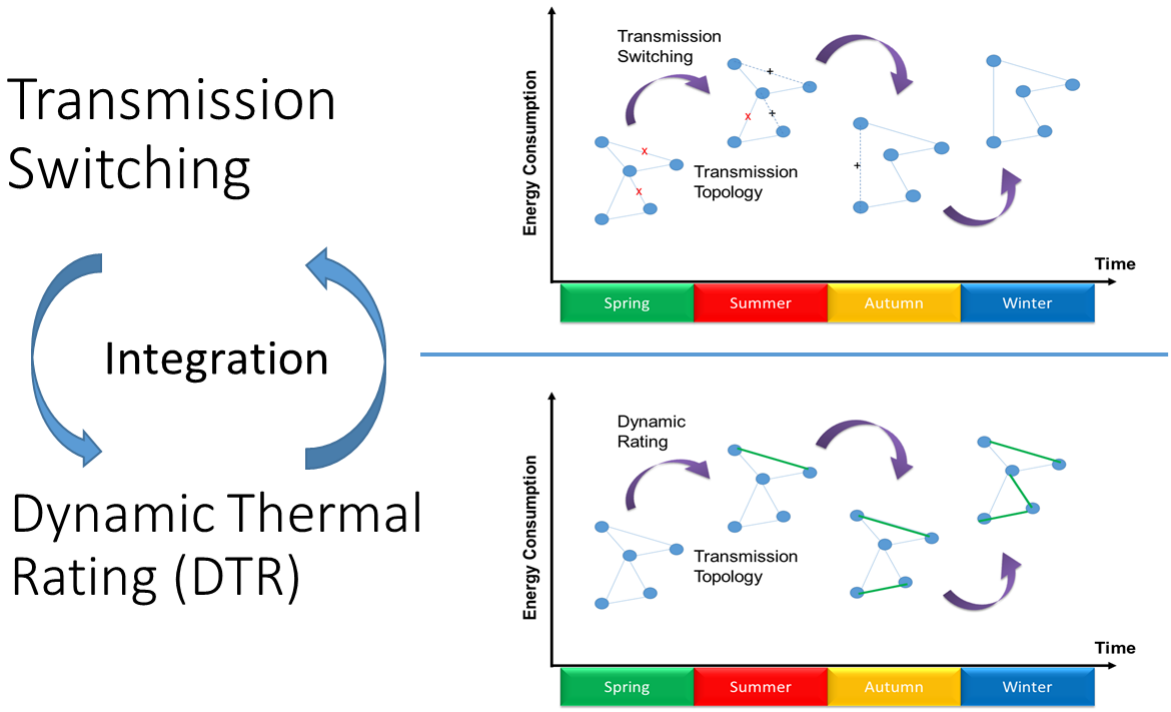


Figure 9: Coordination of Dynamic Thermal Rating with Seasonal Transmission Switching

in cost savings, in practice transmission switching is done mostly for periodic maintenance and planning issues. A periodic transmission switching model is proposed in [14] where the transmission switching occurs at the beginning of a time period (season) and remains unchanged during that period.

Currently, most of transmission systems use static ratings. There are challenges on the way of transmission systems to effectively utilize the dynamic ratings. First, new investments are required on the DTR equipment. It is necessary to develop optimal plans for the gradual integration of the DTR system into the transmission network. Second, monitoring the real-time factors is naturally difficult to be conducted for a high number of transmission lines. Therefore, the DTR system should be targeted toward a few but the most suitable lines. Another challenge is how to coordinate the transmission switching operations with the DTR lines to form a reliable and economic transmission grid (Figure 9). In this chapter, we develop a mixed

integer model to find new investment solutions for the gradual integration of the DTR technology into power systems. Our developed model is multi-stage in which lines can be invested during any time period in the planning horizon. We develop a decomposition algorithm that solves the problem efficiently. The proposed model is unique in terms of the optimal investment planning for the real-time line rating system. To our best knowledge, this problem has not been studied in the literature. We also consider the transmission switching operation with the dynamic rating system. This is the first time both the DTR and TS practices are studied together and their simultaneous economic effects on the power generation and dispatch are investigated.

This chapter is organized as follows. Section 2.3 describes the proposed mathematical programming model. A benders decomposition is developed and described in Section 2.4. Sections 2.5, 2.6, and 2.7 are devoted to conduct experiments of the proposed model and the benders decomposition approach on the Garver's 6-bus and IEEE 118-bus power systems. Section 2.8 gives the conclusions.

## 2.3 The Proposed Model

In this section, we develop a mixed integer linear model for the investment on the dynamic thermal rating and its coordination with the transmission switching. Our model is an extension of the DCOPF model where the thermal capacity of lines are expandable and the transmission topology is switchable. We include N-1 reliability requirements (single contingencies), as in [15], and the variability of loads in different times. Note that single contingencies may refer to failure of a single element (a generator or a transmission line) or simultaneous failure of multiple elements. If there are two or more elements in a power system that are physically or electrically linked, then failure of each of those elements can result in failure of other linked elements. Simultaneous failure of physically or electrically linked elements are also considered as the N-1 contingency scenarios. Since our proposed model is for multi-period planning

purposes, we ignore the temporal constraints for the power generation units such as ramping limits.

We also want to emphasize that the focus of this chapter is the long-term planning for the dynamic thermal rating and to find a few but the best lines for the investment. Although many factors can affect the real-time dynamic ratings of the lines (see equations (4)), the real time thermal capacities of lines in the long term are usually higher than the traditional static ratings [16, 17]. Therefore, we assume that if any line is equipped with the DTR technology, then its dynamic thermal capacity will be higher (e.g. at least 20% or 30%) than its traditional static ratings. This way of simplification results in a computationally tractable model which, at the same time, enables us to detect the most suitable lines for the DTR utilization. Moreover, in the experiments at Section 2.7 (Study 1) we will show that the uncertainties in the real-time capacity of lines actually do not change the identity of the most suitable lines for the DTR investment. It should be also emphasized that if the purpose was to plan for the short-term transmission operations, then it would be better to include the uncertainties of line capacities in the optimization model. The model is described by (5a) to (5o). The brackets next to constraints (5h) to (5o) include corresponding dual variables when the binary decision variables are set to fixed values.

$$\min \quad \sum_{t}\sum_{k}\frac{C_k^{\mathrm{d}}\,x_{tk}}{(1+i)^{t-1}}+\sum_{t}\sum_{l}\sum_{n}\frac{H_l\,C_n^{\mathrm{g}}\,g_{tl0n}}{(1+i)^{t-1}} \tag{5a}$$

Subject to

$$\sum_{t} x_{tk} \le 1 \quad \forall\, k \tag{5b}$$

$$\sum_{k} x_{tk} \le X_t^{\max} \quad \forall\, t \tag{5c}$$

$$\sum_{t}\sum_{k}\frac{C_k^{\mathrm{d}}\,x_{tk}}{(1+i)^{t-1}} \leq I^{\mathrm{d}} \tag{5d}$$

$$\sum_{k}(1-z_{tlk}) \leq Z_{tl}^{\max} \quad \forall\, t,l \tag{5e}$$

$$x_{tk}, z_{tlk} \in \{0,1\} \quad \forall\, t,l,k \tag{5f}$$

$$\sum_{n\in\eta_b} g_{tlrn} + \sum_{k\in\Phi_b^+} f_{tlrk} - \sum_{k\in\Phi_b^-} f_{tlrk} = D_{tlb} \quad \forall\, t,l,r,b \quad [\alpha_{tlrb}] \tag{5g}$$

$$f_{tlrk} - R_{rk}E_k(\theta_{tlra_k} - \theta_{tlrb_k}) \geq -(1-z_{tlk})M_k \quad \forall\, t,l,r,k \quad [\beta_{tlrk}] \tag{5h}$$

$$f_{tlrk} - R_{rk}E_k(\theta_{tlra_k} - \theta_{tlrb_k}) \leq (1-z_{tlk})M_k \quad \forall\, t,l,r,k \quad [\gamma_{tlrk}] \tag{5i}$$

$$-\Theta_k^{\max} \leq \theta_{tlra_k} - \theta_{tlrb_k} \leq \Theta_k^{\max} \quad \forall\, t,l,r,k \quad [\mu_{tlrk},\ \omega_{tlrk}] \tag{5j}$$

$$f_{tlrk} \geq -R_{rk}(F_k^{\mathrm{s}} z_{tlk} + y_{tlrk}) \quad \forall\, t,l,r,k \quad [\delta_{tlrk}] \tag{5k}$$

$$f_{tlrk} \leq R_{rk}(F_k^{\mathrm{s}} z_{tlk} + y_{tlrk}) \quad \forall\, t,l,r,k \quad [\pi_{tlrk}] \tag{5l}$$

$$G_n^{\min} R'_{rn} \leq g_{tlrn} \leq G_n^{\max} R'_{rn} \quad \forall\, t,l,r,n \quad [\upsilon_{tlrn},\ \lambda_{tlrn}] \tag{5m}$$

$$0 \leq y_{tlrk} \leq \Delta F_k^+ \sum_{j=1}^{t} x_{jk} \quad \forall\, t,l,r,k \quad [\rho_{tlrk}] \tag{5n}$$

$$y_{tlrk} \leq \Delta F_k^+ z_{tlk} \quad \forall\, t,l,r,k \quad [\tau_{tlrk}] \tag{5o}$$

The objective function (5a) minimizes the total cost which is comprised of the investment cost on the DTR equipment and the electricity generation cost with no contingency. In the objective function (5a) the electricity generation cost at all hours is calculated as the generation cost of the load blocks multiplied by their durations in

terms of number of hours ($H$). Constraints (5b) ensure that for each line only one-time investment is considered. The constraints (5c) and (5d) enforce the limitations in number of lines to be upgraded and in the investment capital in beginning of the project, respectively. Constraints (5e) limit the number of switched lines at each period to the desired values. Meeting all loads over the planning period is satisfied by constraints (5g). In the power balance constraints (5g), a net load $D$ (i.e. the forcasted load minus the forecasted wind/solar) is considered. The physical relation between the phase angles of connected buses and the power flow in connecting lines are represented by constraints (5h) and (5i). The bounds on the phase angle differences of connected buses are enforced by constraints (5j) and the transmission thermal limits are enforced by constraints (5k) and (5l). The state of binary variable $z$ denotes that a line is in service ($z = 1$) or out of service ($z = 0$). The generators capacity are represented by constraints (5m). Constraints (5n) ensure that dynamic ratings are exploited only on lines with the DTR technology installed. Similarly constraints (5o) make sure that dynamic ratings are used on lines that are in service. Therefore, in constraints (5k) and (5l) either static or dynamic thermal limits are incorporated in the model depending on the values of $y$ and $z$. If a line is not invested with the DTR technology ($y = 0$) and is in service ($z = 1$), then inequalities (5k) and (5l) will constraint the thermal capacity of that line to its static rating $F^{\mathrm{s}}$. Similarly, If a line is invested with the DTR technology ($0 \leq y \leq \Delta F^{+}$) and is in service ($z = 1$), then inequalities (5k) and (5l) will constraint the thermal capacity of that line to its dynamic rating $F^{\mathrm{s}} + \Delta F^{+}$.

To maintain the system reliability at single contingencies in generators or transmission lines, the binary parameters $R$ and $R'$ are used in the model where

$$R_{rk} = \left\{ \begin{array}{ll} 0 & \text{if } r = k \\ 1 & \text{otherwise} \end{array} \right\} \forall\, k, r \qquad R'_{rn} = \left\{ \begin{array}{ll} 0 & \text{if } r = K + n \\ 1 & \text{otherwise} \end{array} \right\} \forall\, n, r \quad (6)$$

A value of $R_{rk} = 0$ means that line $k$ is under contingency and therefore it is not working. Similarly, a value of $R'_{rn} = 0$ means generator $n$ is not working. Constraints (5h) and (5i) include the disjunctive parameter $M$. By setting the value of this parameter to a sufficiently large number, the inequality constraints (5h) and (5i) will be redundant when the corresponding line is switched out of service. However, a lower value for this parameter results in a stronger linear programing relaxation and is, therefore, desirable. In [9] a value of $E_k\Theta_k^{\max}$ is used for the disjunctive parameter. This value can result in significant increase in solution time especially in transmission systems with lines having high electrical susceptance. Tuning the disjunctive parameter for the transmission expansion problem is discussed in [18]. In their method, a shortest or longest path problem is solved for every line to find the minimum value for the disjunctive parameter. This method can be computationally demanding when the size of the transmission network is large (See [18]). In this chapter we propose to use the value of

$$M_k = \max \left\{ \sum_{l \in \left(\Phi^{\pm}_{a_k} \cup \Phi^{\pm}_{b_k}\right)} \left(F^{\mathrm{s}}_k + \Delta F^{+}_k\right) \right\} \tag{7}$$

for the disjunctive parameter for transmission switching. Use of the value (7) results in faster convergence to the optimal solution when compared to the value used in [9] and is also easy to calculate. Exploring the effective values for the disjunctive parameter $M$ is beyond the scope of this chapter and requires more research for new techniques and evaluation of tuning methods, especially in transmission switching and other similar problems.

### 2.4 Developed Benders Decomposition

The problem (5) includes binary decision variables $x$ and $z$ which creates four decision possibilities for every line. If we ignore the case $x = 1$ & $z = 0$, then for a power

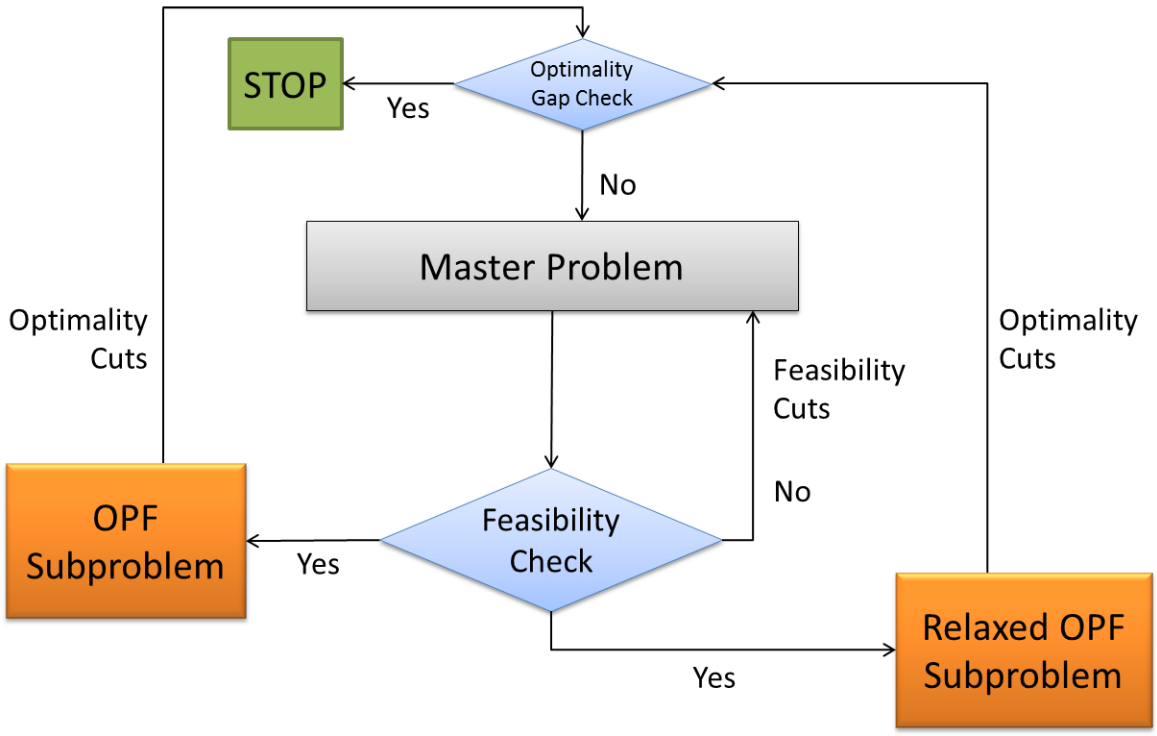


Figure 10: The developed decomposition approach

system with $N$ transmission lines and one period of operation there are $3^N$ alternate topologies. As there are multiple time periods and N-1 reliability constraints, directly solving the problem (5) using a commercial solver is difficult for small power systems and impossible for larger systems because of time and memory inefficiency. To overcome this challenge we develop a benders decomposition approach illustrated in Figure 10. We decompose the problem (5) into a master problem and three subproblem. The goal of the master problem is to find an optimal plan for the investment in the dynamic rating system and also for the transmission switching all through the planning horizon. The solution of the master problem provides a lower bound for the optimal solution. The master problem is formulated by (8a) to (8b). The variable $P$ represents the objective function of the master problem and accounts for the summation of total investment cost in the dynamic rating system and total electricity

generation cost.

$$\text{Master Problem: Min} \quad P \tag{8a}$$

Subject to

$$\text{Constraints } (5b)\text{–}(5f) \tag{8b}$$

When the master problem is solved, its proposed investment and switching plan (solutions $x$ and $z$) are passed to the subproblems. Therefore the subproblems are linear and continuous problems. The first subproblem is the feasibility subproblem and is formulated as (9a) to (9d). The variables $s^+$ and $s^-$ in constraints (9b) represent the amounts of the energy shortage and excess, respectively.

Feasibility Subproblem:

$$\text{Min} \quad \sum_t \sum_l \sum_r \sum_b (s^+_{tlrb} + s^-_{tlrb}) \tag{9a}$$

Subject to

$$\sum_{n \in \eta_b} g_{tlrn} + \sum_{k \in \Phi^+_b} f_{tlrk} - \sum_{k \in \Phi^-_b} f_{tlrk} + s^+_{tlrb} - s^-_{tlrb} = D_{tlb} \quad \forall\, t, l, r, b \quad [\alpha'_{tlrb}] \tag{9b}$$

$$\text{Constraints } (5h)\text{–}(5o) \tag{9c}$$

$$s^+_{tlrb}, s^-_{tlrb} \geq 0 \quad \forall\, t, l, r, b \tag{9d}$$

The feasibility subproblem has at least one feasible solution. This is because if we set the value of variables $f$, $\theta$, and $y$ to 0 and $g$ to $G^{\min}$, it results in a feasible energy balance of $\sum_{n \in \eta_b} G^{\min} + 0 - 0 + s^+_{tlrb} - s^-_{tlrb} = D_{tlb}$ where all other constraints

are satisfied. Therefore, the dual of the feasibility subproblem is bounded and has an optimal solution. This property enables us to directly use the solution of the feasibility subproblem to evaluate the security of the proposed plan by the master problem. To check weather the proposed plan satisfies all the operation constraints, the feasibility subproblem calculates the amount of the energy mismatches and minimizes them. This way, the feasibility subproblem preserves the power balance at every bus under both non-contingency and contingency scenarios at all time periods. In the case of energy mismatch (shortage or excess), the feasibility cut (10) is calculated using the dual solutions of the feasibility subproblem and is added to the master problem.

$$\begin{aligned}\sum_{t}\sum_{l}\sum_{r}\Bigg(&\sum_{b}\alpha'_{tlrb}D_{tlb}-\sum_{k}\beta_{tlrk}(1-z_{tlk})M_k+\sum_{k}\gamma_{tlrk}(1-z_{tlk})M_k\\&-\sum_{k}\mu_{tlrk}\Theta_k^{\max}+\sum_{k}\omega_{tlrk}\Theta_k^{\max}\\&-\sum_{k}\delta_{tlrk}R_{rk}F_k^{\mathrm{s}}z_{tlk}+\sum_{k}\pi_{tlrk}R_{rk}F_k^{\mathrm{s}}z_{tlk}\\&+\sum_{n}\upsilon_{tlrn}G_n^{\min}R'_{rn}+\sum_{n}\lambda_{tlrn}G_n^{\max}R'_{rn}\\&+\sum_{k}\sum_{j=1}^{t}\rho_{tlrk}\Delta F_k^{+}x_{jk}+\sum_{k}\tau_{tlrk}\Delta F_k^{+}z_{tlk}\Bigg)\leq 0\end{aligned}\tag{10}$$

In the feasibility cut (10), the parameters $\alpha'$ are the dual values of power balance constraints (9b). The $\beta$ and $\gamma$ are the dual values of power flow constraints (5h) and (5i), respectively. Parameters $\mu$ and $\omega$ represent the dual values of the min and max phase angle differences (5j), respectively, and $\delta$ and $\pi$ as the dual values of min thermal capacity (5k) and max thermal capacity (5l) constraints, respectively. The $\upsilon$ and $\lambda$ are the dual values of the min and max generation capacity constraints (5m), respectively, the $\rho$ represent the dual values of the constraints (5n), and finally $\tau$

represent the dual values for the constraints (5o). An energy mismatch (shortage or excess) means a positive objective function value for the feasibility subproblem (9). Because of the strong duality theory, the left hand side of the feasibility cut (10) is equal to the objective function of the feasibility subproblem (9). If the proposed plan (solutions $x$ and $z$) result in the energy mismatch, then they are cut off from the solution space of the master problem by restricting the left hand side of the feasibility cut (10) to non-positivity and adding it to the master problem. If the proposed plan is feasible (zero energy mismatch), the feasibility subproblem passes the proposed feasible plan to two optimality subproblems. The first optimality subproblem is the OPF subproblem and is formulated as (11a) to (11b).

$$\text{OPF Subproblem: Min} \quad \sum_{t}\sum_{l}\sum_{n}\frac{H_l\, C_n^{\mathrm{g}}\, g_{tl0n}}{(1+i)^{t-1}} \tag{11a}$$

$$\text{Subject to}$$

$$\text{Constraints } (5g)\text{–}(5o) \text{ with } r=0 \tag{11b}$$

To check the optimality of the proposed plan, the OPF subproblem calculates the energy generation cost only for the non-contingency scenario and minimizes it. The total energy generation cost of the OPF subproblem along with the total DTR investment cost are used to calculate the upper bound of the optimal solution. After the OPF subproblem is solved, its dual solutions are used to form benders optimality cut (12) which is added to the master problem.

$$\begin{aligned} P \quad \geq \quad & \sum_{t}\sum_{k}\frac{C_k^{\mathrm{d}} x_{tk}}{(1+i)^{t-1}} \\ & + \sum_{t}\sum_{l}\sum_{r}\left(\sum_{b}\alpha_{tlrb} D_{tlb}\right. \end{aligned}$$

$$
\begin{aligned}
&- \sum_{k} \beta_{tlrk}(1 - z_{tlk}) M_k + \sum_{k} \gamma_{tlrk}(1 - z_{tlk}) M_k \\
&- \sum_{k} \mu_{tlrk} \Theta_k^{\max} + \sum_{k} \omega_{tlrk} \Theta_k^{\max} \\
&- \sum_{k} \delta_{tlrk} R_{rk} F_k^{\mathrm{s}} z_{tlk} + \sum_{k} \pi_{tlrk} R_{rk} F_k^{\mathrm{s}} z_{tlk} \\
&+ \sum_{n} \upsilon_{tlrn} G_n^{\min} R'_{rn} + \sum_{n} \lambda_{tlrn} G_n^{\max} R'_{rn} \\
&+ \sum_{k} \sum_{j=1}^{t} \rho_{tlrk} \Delta F_k^{+} x_{jk} + \sum_{k} \tau_{tlrk} \Delta F_k^{+} z_{tlk} \Bigg) \qquad (12)
\end{aligned}
$$

In the optimality cut (12), parameters $\alpha$ are the dual values of power balance constraints (5g). The remaining parameters $\beta$, $\gamma$, $\mu$, $\omega$, $\delta$, $\pi$, $\upsilon$, $\lambda$, $\rho$, and $\tau$ are defined in the same way they were defined at the feasibility cut (10). The right hand side of the optimality cut (12) is the summation of total investment cost in the dynamic rating system and total electricity generation cost. The solution time for the decomposition algorithm can be improved by generating more optimality cuts. A second optimality subproblem is defined to provide extra optimality cuts to the master problem and accelerate the convergence to the optimal plan. The second subproblem is obtained from the OPF subproblem by relaxing the constraints (5h) to (5j) and is called the relaxed OPF subproblem (ROPF). The ROPF subproblem is formulated as (13a) to (13b).

$$
\text{ROPF Subproblem: Min} \quad \sum_{t} \sum_{l} \sum_{n} \frac{H_l \, C_n^{\mathrm{g}} \, g_{tl0n}}{(1+i)^{t-1}} \qquad (13a)
$$

Subject to

$$
\text{Constraints } (5g) \text{ and } (5k)\text{–}(5o) \text{ all with } r = 0 \qquad (13b)
$$

The optimality cut (14) is constructed using the dual solutions of the ROPF subproblem and is added to the master problem. In the optimality cut (14), parameters $\alpha$ are again the dual values of power balance constraints (5g). The parameters $\delta$, $\pi$, $\upsilon$, $\lambda$, $\rho$, and $\tau$ are defined in the same way they were defined at the feasibility cut (10). As the ROPF subproblem does not include the disjunctive parameter, its optimality cut (14) further narrows down the search space of the master problem. The relaxed subproblems are also used in the transmission expansion problem (e.g. see [18]).

$$
\begin{aligned}
P \quad \geq \quad & \sum_{t}\sum_{k}\frac{C_k^{\mathrm{d}}x_{tk}}{(1+i)^{t-1}} \\
& + \sum_{t}\sum_{l}\sum_{r}\Bigg(\sum_{b}\alpha_{tlrb}D_{tlb} \\
& \qquad - \sum_{k}\delta_{tlrk}R_{rk}F_k^{\mathrm{s}}z_{tlk} + \sum_{k}\pi_{tlrk}R_{rk}F_k^{\mathrm{s}}z_{tlk} \\
& \qquad + \sum_{n}\upsilon_{tlrn}G_n^{\min}R'_{rn} + \sum_{n}\lambda_{tlrn}G_n^{\max}R'_{rn} \\
& \qquad + \sum_{k}\sum_{j=1}^{t}\rho_{tlrk}\Delta F_k^{+}x_{jk} + \sum_{k}\tau_{tlrk}\Delta F_k^{+}z_{tlk}\Bigg)
\end{aligned}
\tag{14}
$$

Our solution approach for the optimal planning is summarized as the following procedure.

1. Set the lower and upper bound of the problem to minus and plus infinity, respectively. Solve the master problem and calculate the dynamic rating and switching plan. Update the lower bound of the problem to the objective value of the master problem. Pass the proposed plan to the feasibility subproblem.

2. Solve the feasibility subproblem and calculate the energy mismatch for the proposed plan. If the proposed plan is secure, pass the feasible plan to the optimality subproblems and proceed to the next step. Otherwise, add the feasibility cut to the master problem and go to step 1.

3. Solve the OPF subproblem and add its optimal power generation cost to the investment cost for the proposed dynamic rating plan. Consider the total cost as the updated upper bound of the problem.

4. If the difference between the upper bound and the lower bound is larger than the pre-specified threshold, add the optimality cuts of the OPF and ROPF subproblems to the master problem and return to the step 1. Otherwise, consider the current proposed plan as optimal.

Note that the developed decomposition algorithm is an accelerated version of benders partitioning procedure [19] for solving the mixed integer problem (5). The master problem (8) is actually a relaxed version of the problem (5). Because the master problem (8) is a pure integer linear program, its optimal solution is one of the vertices in its convex hull and can be found in finite number of steps using the branch and bound or any other discrete optimization algorithm. The subproblems (9), (11), (13) are bounded linear programs with convex solution spaces . At each iteration of the decomposition algorithm, one vertex of the feasibility or optimality subproblem is used to form a feasibility or optimality cut. The formed cut is a linear constraint with integer variables $x$ and $z$ added to the master problem. Therefore, the convex hull of the master problem may shrink to a smaller convex hull which contains an updated optimal solution to the master problem. As there are finite number of vertices at the solution spaces of the subproblems, the decomposition algorithm will converge to the global optimal solution at representative load vectors in finite number of iterations.

Table 7: Load profile in one year

| | Q1 | Q2 | Q3 | Q4 |
|---|---|---|---|---|
| Load Block Low | 0.47 | 0.44 | 0.41 | 0.41 |
| Duration (h) | 748 | 749 | 762 | 765 |
| Load Block Avg. | 0.71 | 0.67 | 0.63 | 0.63 |
| Duration (h) | 720 | 728 | 736 | 736 |
| Load Block High | 0.92 | 1.0 | 0.84 | 0.84 |
| Duration (h) | 692 | 707 | 710 | 707 |

## 2.5 Numerical Experiments

The investment model is studied on two test power systems: the Garver's system (Section 2.6) and the IEEE 118-bus system (Section 2.7). In all studies, a value of $\pm 1.2$ radians is considered for minimum/maximum phase angle differences. The DTR equipment prices collected in [20] are used to estimate the investment costs. The installation, maintenance, and transmission switching costs are ignored. As the installation time for the DTR equipment is short [21], the outage time for lines under the equipment installation is not considered. The PJM hourly load data [22] for sub-zone PN for year 2011 is normalized by scaling between 0 and 1 and then the normalized data is multiplied by the system load to generate demand in different hours of the year. A load growth rate is used to estimate the future loads. To reduce the size of the problem, a year is divided to four quarters and each quarter is divided to three load blocks of low, average, and high. The profile of loads is provided in Table 7. The number of loads falling in each load block is considered as the duration of that load block and is used in the cost weight vector $H$. An unlimited budget for the capital dynamic rating investment is assumed. All recurring costs, including operational and investment, are assumed to be the same in future time periods. The decomposition algorithm is coded in C++ and Gurobi is used to solve LPs and MIPs.

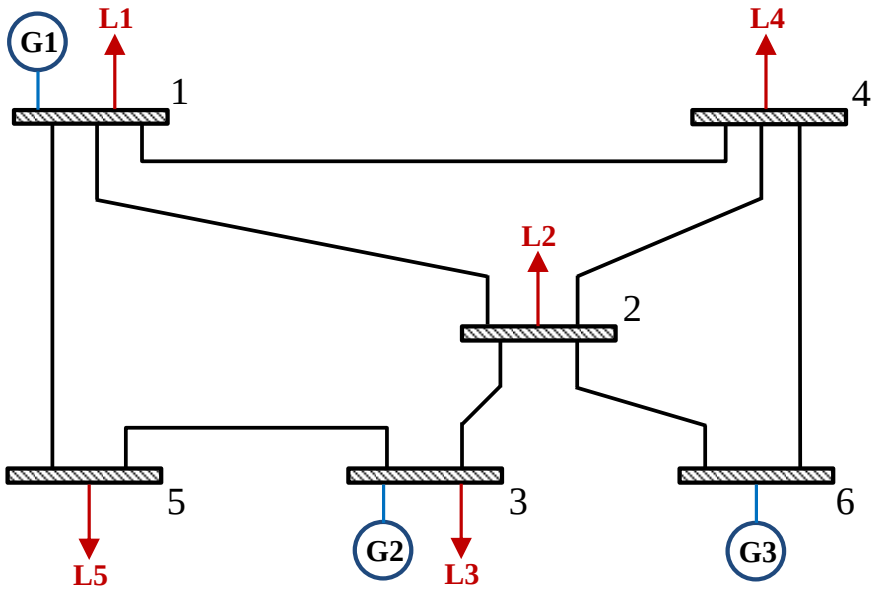


Figure 11: The Garver's system

We use a computer model with Intel(R) Celeron(R) CPU 1005M @ 1.90GHz and 4GB of RAM memory to calculate the results.

In a study in California [16] is is reported that, in times, the dynamic rating can be 150% more than the static rating. The study indicates that, in overall and for the specific monitored transmission lines, real-time line ratings provide 40% to 80% more capacity than the static transmission line ratings. In another case study conducted in Southeast France [17] it is concluded that setting the maximum thermal capacity to 30% above static ratings resulted in a usability of 92.1% for the transmission system, i.e. in 92.1 percent of the time the predicted DTRs were either correct providing increased capacity for the grid or not correct but requiring no mitigation. For the investment plan calculations we consider conservative increases of 20% and 30% in transmission capacity of lines that are equipped with the DTR technology. Depending

Table 8: Load and generation data for Garver's system

| Bus No. | Load (MW) | Generating Capacity (MW) | Operation Cost ($/MW·h) |
|---|---|---|---|
| 1 | 32 | 150 | 9 |
| 2 | 96 | – | – |
| 3 | 16 | 360 | 7 |
| 4 | 64 | – | – |
| 5 | 96 | – | – |
| 6 | – | 600 | 4 |

on the forecasted ambient conditions surrounding the lines, the amount of increase in the transmission capacity can be readjusted.

### 2.6 Garver's System

The Garver's system in [23] is modified in this study and is illustrated in Figure 11. In the modified system we combine the generators in each bus into one generation unit and change the loads which are provided in Table 8. To connect bus 6 to the network, we assume lines 2–6 and 4–6 are already constructed and available for operations. The data for the transmission lines is provided in Table 9. For the modified Garver's system, it is assumed that $E = 50/X$. Also an investment cost of $50,000 is considered for every line. The lines 1–5, 2–3, 2–6, and 4–6 are considered as candidate lines for the DTR investment. For each invested line, 130% of the static rating is utilized. Lines 1–2, 1–4, 2–3, and 2–4 are considered switchable. Following studies are conducted:

- Study 1: Sensitivity of the investment plan to uncertainties in discount and load growth rates is investigated.

Table 9: Transmission line data for Garver's system

| From | To | X (p.u.) | Capacity (MW) |
|---|---|---|---|
| 1 | 2 | 0.4 | 100 |
| 1 | 4 | 0.6 | 80 |
| 1 | 5 | 0.2 | 100 |
| 2 | 3 | 0.2 | 100 |
| 2 | 4 | 0.4 | 100 |
| 2 | 6 | 0.3 | 100 |
| 3 | 5 | 0.2 | 100 |
| 4 | 6 | 0.3 | 100 |

- Study 2: An investment plan for three years is calculated and results are analyzed.
- Study 3: Contributions of the TS and the DTR to the economy of the power dispatch is analyzed.

The studies are provided in the following.

### 2.6.1 Study 1

In the sensitivity analysis, one year (4 quarters) planning horizon is considered. The discounting rate and the load growth rate are selected as the changing input factors. The total investment and electricity generation cost, the amount of the cost reduction (saving), number of lines invested, and number of lines switched over one year of operation (4 quarters) are considered as the output factors. The base values of 8% for the discounting rate (compounded quarterly) and 2% for the load growth rate are considered and then they are increased/decreased by $\pm 10\%$ of their base value. When changing the value of one input factor, the other input factor is fixed to its base value. Sensitivity plots are provided in Figure 12.

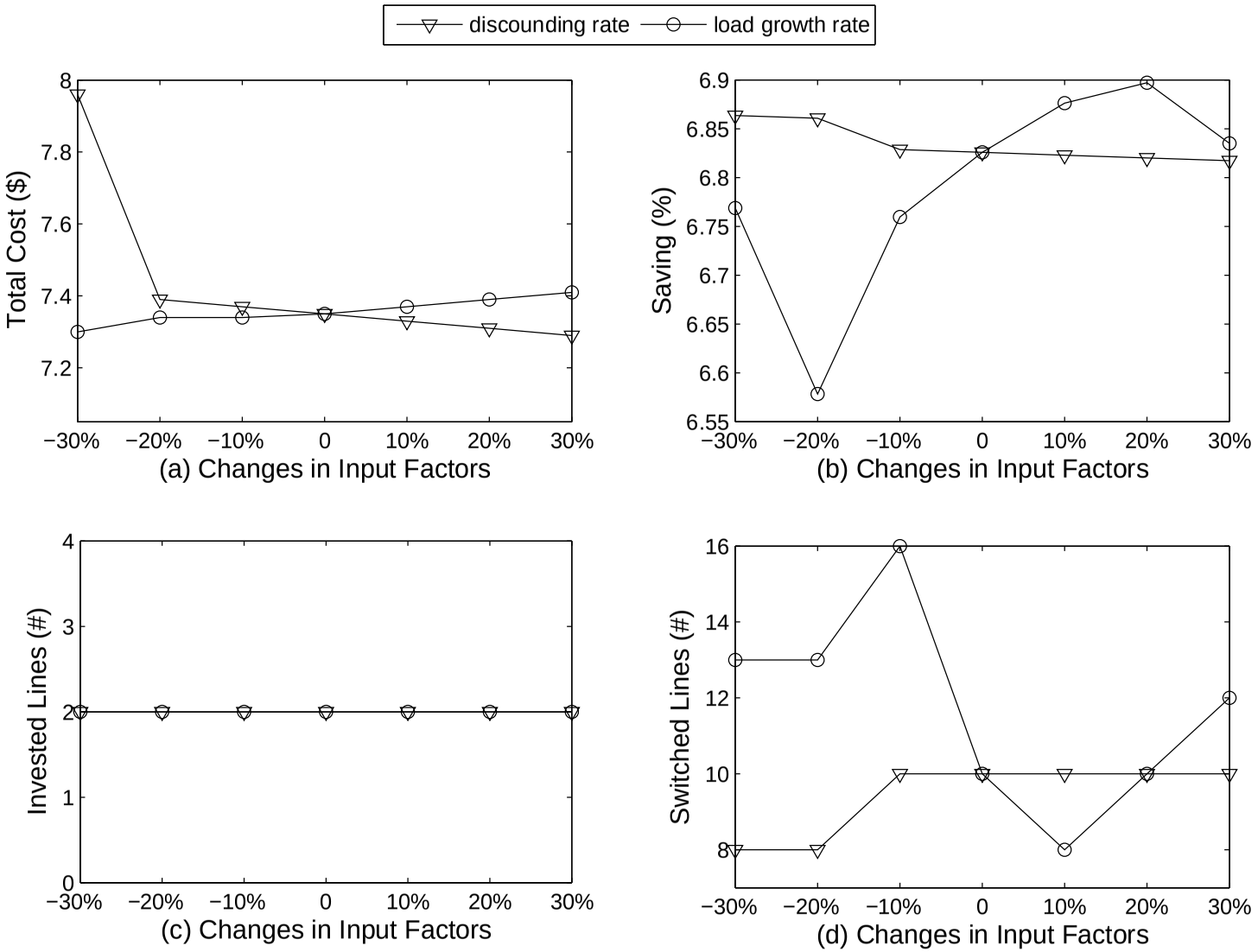


Figure 12: Sensitivity plots (study 1)

As Figure 12a shows, the total cost is negatively sensitive to changes in the discounting rate. This is true as by increasing the value of the discounting rate, the present worth of costs incurring in later quarters decline. The cost is positively sensitive to changes in the load growth rate as it requires more usage of generators' capacity. The percentage of reduction in cost (saving) is sensitive to the load growth rate but not much to the discounting rate (Figure 12b). Totally the increase of the load growth rate from 1.6% (20% below 2%) to 2.4% (20% above 2%) results in 0.32% increase in the saving. This can be explained by the increase in the usage of lines' total capacity when the demand for the electricity increases. This results in more supply of the electricity from cheaper sources of the energy generation. The investment plan is not sensitive to the changes in the discounting and load growth rates. Figure 12c shows that in all considered sensitivity scenarios, two lines are invested and equipped with the dynamic rating technology. The switching plan changes in almost every sensitivity scenario for the load growth rate and in some scenarios for the discount rate (Figure 12d). The lowest number of switches occurs in -30%, and -20% of the base discount rate and also in 10% of the base load growth rate where totally 8 lines are switched out of service in 12 load blocks. The highest case occurs in -10% of the base load growth rate with totally 16 lines removed from service in different load blocks.

### 2.6.2 Study 2

In this case study, a 3-year planning horizon is considered. An annual discounting rate of 8% and an annual load growth rate of 2% is considered. The discounting rate is compounded quarterly. The load growth in first year is assumed to be 0. If no investment is made on the dynamic rating and no transmission switching is practiced, total electricity generation cost over 3 years of operation is $21,895,228 to supply the demand. With investing on the DTR and with practicing TS, total cost decreases to

Table 10: Investment plan and Usability (Study 2)

| Line | Invested Quarter | Invested Capacity | Normal Usability | | | Under N-1 Usability |
|---|---|---|---|---|---|---|
| | | | Min | Avg | Max | |
| 2–6 | 1 | 20MW | 0% | 47.1% | 100% | 0% |
| 4–6 | 1 | 20MW | 0% | 23.6% | 95.4% | 0% |
| 2–3 | 2 | 20MW | 0% | 0% | 0% | 0.32% |

Table 11: Switching plan (Study 2)

| Line | Quarter |
|---|---|
| 1–2 | 1, 2, 3, 4, 5, 6, 7, 8, 9, 10, 11, 12 |
| 1–4 | 1, 7 |
| 2–3 | 2, 3, 11 |
| 2–4 | 2, 3, 4, 5, 6, 8, 9, 10, 11, 12 |

$20,238,167. This is a $1,657,061 reduction in cost which accounts for 7.57% saving. This saving is significant especially for a very small power system like Garver's system and can be bigger for larger power systems. The investment solutions are provided in Table 10 and the switching solutions in Table 11. Totally $150,000 is invested on the DTR equipment for 3 lines. At the beginning of the investment plan, lines 2–6 and 4–6 are equipped with the DTR technology to transmit more power flow from the cheapest generating unit (unit at bus 6) to supply loads at buses 2 and 4 and others. In the first quarter the other lines do not reach their static thermal limits and no further investment is made. Starting from quarter 2 at all high load blocks, extra transmission capacity is required for line 2–3 to maintain the system reliability at N-1 contingencies. Therefore, the DTR technology is installed on this line in second quarter to protect the system reliability while the load is high.

The "usability" of the dynamic ratings on invested lines are also analyzed in Table 10. We define "usability" as the average percentage of the minimum additional thermal capacity $\Delta F_k^+$, provided by the dynamic rating, that is actually used in the power dispatch operation. In normal operations and on average, the minimum additional thermal capacity for line 2–6 is used the most when compared to other lines (47.1% of 20MW), and in 33.3% of times it is fully exploited. In terms of the usability of the minimum additional capacity in normal operations, lines 4–6 is ranked second. In the operations without contingency the minimum additional capacity for Line 2–3 is never used. However 0.32% of the minimum additional capacity for line 2–3 is used in contingency conditions to avoid unmet demand. Line 2–3 plays more critical role than lines 2–6 and 4–6 in contingency scenarios. In summary, line 2–6 has the most usability in operations with contingency and line 2–3 in operations without contingencies. From 1st to 12th quarter, totally 27 transmission switching is planned for 4 lines to relieve the congestion. Line 1–2 is switched out of service at every quarter. Line 2–3 is the only line that is part of both the investment plan and the switching plan. The number of switches for 1st, 2nd and 3rd years are 10, 8, and 9 switches respectively. As was the case in Study 1, there is no stable decrease or increase in number of switches when the electricity demand slightly grows.

### 2.6.3 Study 3

In this study the contributions of DTR and TS approaches on the cost reduction are investigated. The Garver's system becomes infeasible for the annual load growth rates beyond 4%. Therefore for the cost reduction analysis, a load growth range of 0% to 4% with 1% increments is considered. At each experiment, one year of operation (4 quarters) is simulated and cost-related data under four following cases are collected: no DTR and no TS, TS but no DTR, DTR but no TS, both DTR and TS. The same discounting rate of 8% is used. The collected data are summarized in

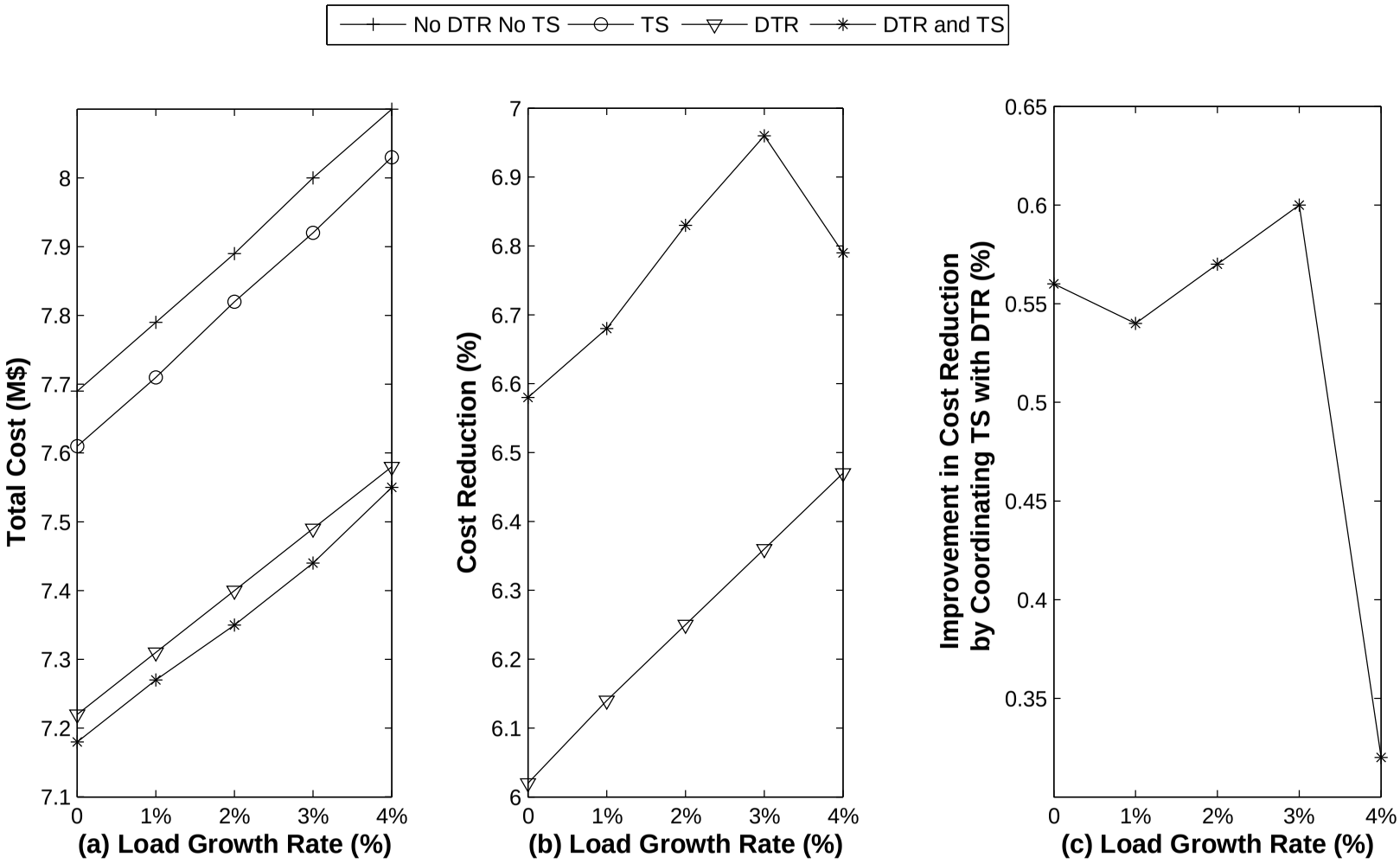


Figure 13: Contributions of DTR and TS to Cost Reduction (Study 3)

Figure 13. Figure 13a shows that the electricity generation cost is the lowest when the DTR approach is integrated with TS approach. If the DTR is considered but not TS, then there is an increase in cost through all load growth rates. Conversely, if TS is practiced without using the DTR, there is even higher increase in costs. The worst case is when none of the DTR and TS approaches are exercised. In this experiment transmission switching does not reduce costs as much as the dynamic rating, however it complements the savings. This is specifically shown in Figures 13b and 13c. The best contribution of TS in cost savings occurs in the experiment with 3% load growth. In that experiment the DTR without TS saves 6.36%. When the DTR is integrated with TS, the saving reaches to 6.96%.

### 2.7 IEEE 118-bus System

Data for the IEEE 118-bus power system is downloaded from [24] where generators' capacity, generation costs, transmission network and line characteristics are taken from [9]. The system is summarized in Table 12. Without using the dynamic rating system and transmission switching, the 118-bus system is not reliable to the single contingency scenarios if one of the generators or lines in Table 13 is lost. To make the system survive in N-1 scenarios and therefore be able to calculate the generation costs, the generators and transmission lines listed in Table 13 are removed from the N-1 contingency list. The generation costs for the 118-bus system are on the order of 50 to 100 times smaller than typical generator costs. We use these costs to be consistent with the results and developed models published in the literature. Therefore, for this power system we consider a lower DTR investment cost of $1000 for every line. All lines are considered as candidate lines for the DTR investment. Following studies are conducted :

- Study 1: Sensitivity of a 3-year investment plan to uncertainties in real-time thermal ratings is investigated.

Table 12: Data for IEEE 118-bus system

| | | Capacity (MW) | | | Cost ($/MWh) | |
|---|---|---|---|---|---|---|
| | No. | Total | Min | Max | Min | Max |
| Generators | 19 | 5859 | 100 | 805 | 0.1897 | 10 |
| Transmission | 186 | 49720 | 220 | 1100 | | |
| Load | 99 | 4519 | 2 | 440 | | |

Table 13: Elements in the 118-bus system removed from the N-1 contingency list

| Generators | Transmission Lines | | |
|---|---|---|---|
| 13 | (12-117) | (14-15) | (16-17) |
| 14 | (18-19) | (29-31) | (68-116) |
| 15 | (71-73) | (77-82) | (82-83) |
| 17 | (83-85) | (84-85) | (85-86) |
| | (85-88) | (85-89) | (86-87) |
| | (88-89) | (89-90) | (89-92) |
| | (90-91) | (91-92) | (110-112) |

- Study 2: The amount of the hourly cost reduction achieved by using the dynamic rating system with and without transmission switching is studied and contributions of both approaches to the economy of the power dispatch are analyzed.

- Study 3: A 1-year investment plan for the dynamic rating system, combined with transmission switching, is calculated and results are analyzed.

The studies are provided in the following.

### 2.7.1 Study 1

The goal of the sensitivity analysis in this study is to investigate the effects of the uncertainty in dynamic thermal ratings (as the input factor) on the candidacy of

lines for investment, investment timing, and the total cost (output factors). In our sensitivity analysis transmission switching is not allowed and maximum two lines per quarter are allowed for investment in the dynamic rating system. For each DTR line at each period, 140% of the static rating is considered as the base for the uncertain dynamic rating and is increased/decreased by ±10% increments. Three years of operation (totally 12 quarters) is considered for the planning horizon. The discounting rate is fixed to 8% compounded quarterly and the annual load growth rate is set to 2%. The high load blocks in Table 7 are considered as quarterly demands for electricity with durations 2160, 2184, 2208, and 2208 for 1st, 2d, 3rd, and 4th quarters, respectively. The results are summarized in the sensitivity plots in Figure 14.

The results in Figure 14(a) shows that the investment plan for the utilization of the dynamic ratings is not much sensitive to changes in dynamic ratings and is composed of a few certain lines. Totally 8 transmission lines are invested in different scenarios when the predicted dynamic ratings are increasing from 110% to 170% of the static ratings. Lines 116, 134, and 154 are invested at all scenarios. Lines 141 and 142 are part of the investment plan in all cases except in 110% scenario. Lines 42 and 113 are invested at 5 scenarios and line 120 only at 170% scenario. Figure 14(b) explores the changes in investment timings for three most invested lines 116, 134, and 154. Under all scenarios, the investment time for line 134 is set to first quarter. Line 154 is always invested at second quarter except under 150% scenario. The investment plan for line 116 is sensitive to changes in dynamic ratings. For instance, as the line rating scenarios increase to 150% or beyond, the investment time for line 116 is advanced from fifth quarter to first quarter. In other scenarios, the investment times for line 116 are oscillating between first to sixth quarters. Figures 14(c) and 14(d) indicate that the number of invested lines increases from 3 lines to 7 lines and total cost deceases from $30,423,627 to $27,716,595 when the line ratings become higher. These

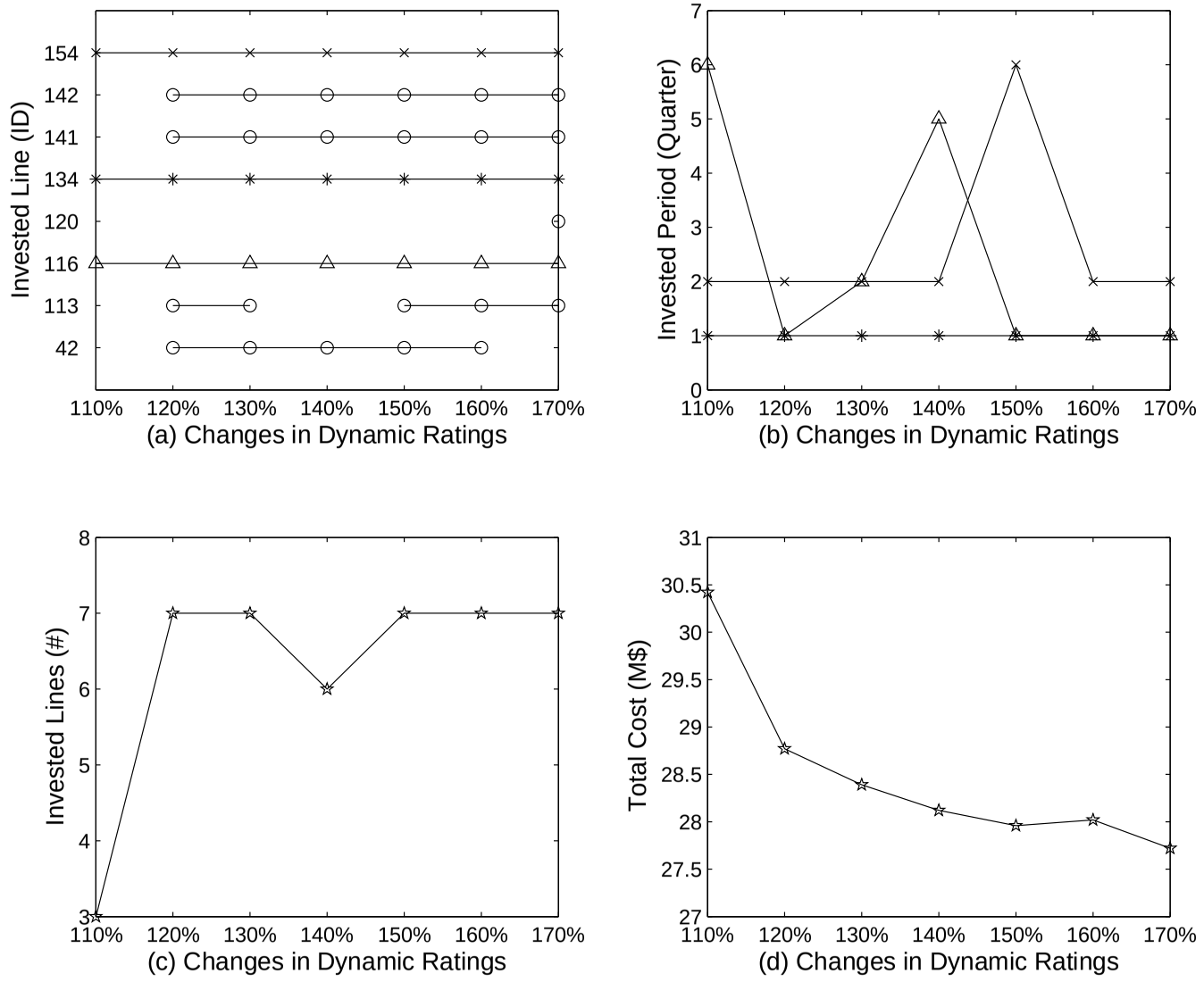


Figure 14: Sensitivity plots (study 1)

changes are expected as the amount of cost savings resulting from higher dynamic ratings gradually justify the initial investment costs in the DTR system. Also the load growth factor creates more power demand in second and third years which in return requires investment in more lines' dynamic capacity at early quarters.

### 2.7.2 Study 2

In the second study, we do not consider the investment cost and only focus on the power generation cost. The purpose of this study is to see how much operational cost in one hour with system load can be reduced by utilizing the dynamic rating system and by integrating the DTR with TS. For each DTR line the 120% of the static ratings are considered to be utilized. Different scenarios for the number of lines equipped with the dynamic rating system ($N_{\text{DTR}}$) and number of switched lines ($N_{\text{TS}}$) are considered and the resulting costs are summarized in Table 14. If dynamic ratings are not utilized and transmission switching is not practiced, total electricity generation cost to supply one hour system load is \$2,054. If the dynamic rating system is used for line 154, it results in the \$188/hr reduction in the cost which is 9.13% saving per hour. Utilizing the DTRs in lines 134 and 154 results in a higher saving of 20.25% per hour. If three or four lines are considered for the DTR, the amount of savings increase slightly. However, when five lines are considered, then total cost decreases to \$1,535/hr. This is a \$519/hr reduction in the cost which accounts for 25.31% saving per hour. The total cost slightly decreases to \$1,533/hr (\$2 more reduction) when 7 lines are considered. There is no more improvement in the cost reductions when the dynamic ratings are utilized on more than 7 lines (See Figure 15).

The studies in [9, 25] show that the majority of the cost savings resulting from transmission switching comes from switching a few lines. To improve the computational efficiency, the switchable transmission lines are limited to lines 38, 62, 64, 78,

Table 14: Costs with DTR and with TS (Study 2)

| Only DTR | | DTR Integrated with TS | | |
|---|---|---|---|---|
| $N_{\text{DTR}}$ | Cost | $N_{\text{DTR}}$ | $N_{\text{TS}}$ | Cost |
| 0 | \$2054 | 0 | 0 | \$2054 |
| 1 | \$1867 | 1 | 1 | \$1683 |
| 2 | \$1638 | 2 | 2 | \$1561 |
| 3 | \$1626 | 3 | 3 | \$1519 |
| 4 | \$1626 | 4 | 4 | \$1509 |
| 5 | \$1535 | 5 | 5 | \$1500 |
| 6 | \$1535 | 5 | 6 | \$1494 |
| 7 | \$1533 | 5 | 7 | \$1466 |
| – | – | 5 | 8 | \$1438 |

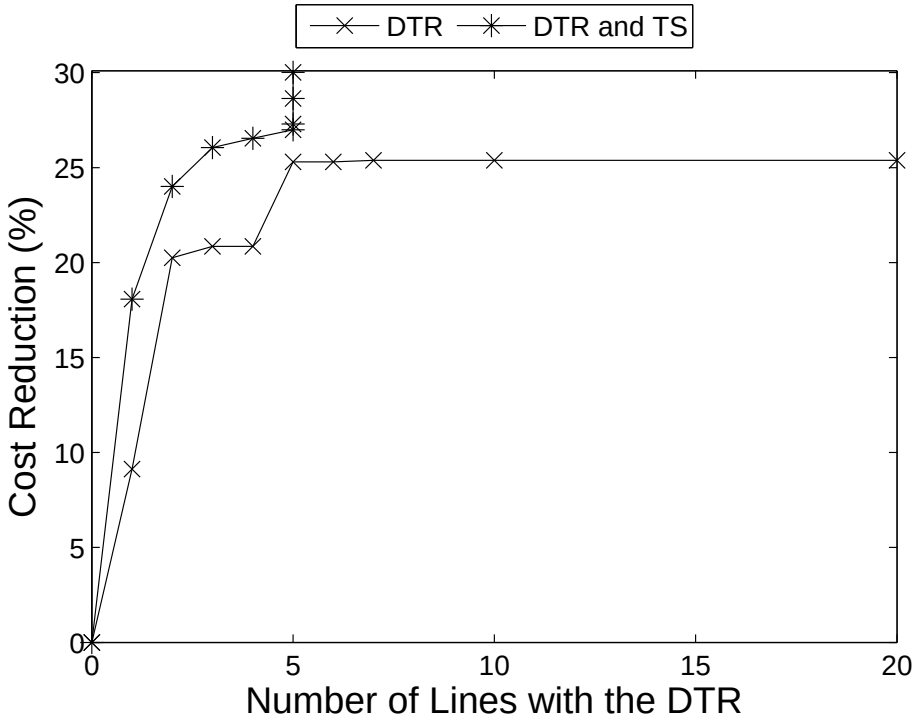


Figure 15: Cost Reductions (Study 2)

118, 132, 133, 143, 153, and 170. In the next analysis, the DTR is integrated with the TS and the results are summarized in 3rd to 5th columns of Table 14. The electricity generation cost decreases more when the DTR system is integrated with TS. When line 132 is switched out of service along with utilization of the DTR in line 154, the electricity generation cost reduces from \$1,867 to \$1,683. In experiments with only the dynamic rating system, the lowest obtained cost is \$1,533 which is achieved by utilizing the DTR of 7 lines. The same cost can be achieved by utilizing the DTR of 2 or 3 lines while 2 or 3 lines are switched out of service (See Table 14 where $N_{\text{DTR}} = N_{\text{TS}} = 2$ and $N_{\text{DTR}} = N_{\text{TS}} = 3$). The lowest cost of \$1,438 per hour occurs in the experiment with 5 lines using the dynamic rating system while 8 lines are switched out of service. This is a 30% reduction in the electricity generation cost in one hour. This study indicates three results on the 118-bus system: 1) the utilization of the dynamic rating system significantly decreases the electricity generation costs. 2) transmission switching complements the reductions in the costs obtained by the dynamic rating system. 3) practicing transmission switching reduces the number of lines to be invested for utilization of the dynamic rating system (see Figure 15).

### 2.7.3 Study 3

In this study, the potential of the dynamic rating system in transferring power from free and environmentally desirable sources of energy to other areas is examined. We add two 450MW new generation units (NGU1 and NGU2) to buses 1 and 50, respectively, where both units have zero generation costs (like wind or solar). The new generation units NGU1 and NGU2 are excluded from the N-1 contingency list. To obtain the investment plan in a reasonable time, a planning horizon of one year (4 quarters) is selected with an annual discounting rate of 10%, compounded quarterly. The 110% of the average load blocks in Table 7 are used as the quarterly demand profiles with durations 2160, 2184, 2208, and 2208 for 1st, 2d, 3rd, and 4th quarters,

Table 15: Investment and switching plans (Study 3)

| Quarter | Invested Lines | Invested Capacity | Switched Lines |
|---|---|---|---|
| 1 | 80, 134 | 572MW | 132, 133 |
| 2 | 2, 14 | 572MW | 132, 133 |
| 3 | 116, 141 | 572MW | 38, 132, 133 |
| 4 | 112 | 572MW | 78, 143 |

respectively. For each invested line, 130% of the static ratings are utilized. In each quarter, up to 2 lines are allowed for the DTR investment and lines 38, 78, 132, 133, and 143 are considered switchable. The optimality gap for the decomposition algorithm is set to 1%. The detail of the calculated investment and switching plans are summarized in Table 15.

In the optimal plan totally $7,000 is invested on the DTR equipment for lines 2, 14, 80, 112, 116, 134, and 141. With investing on the DTR of those lines and with practicing TS on lines 38, 78, 132, 133, and 143, the total electricity generation cost to supply the demand over one year is $4,391,683. If no investment is made on the dynamic rating and no transmission switching is practiced, then total cost increases to $4,829,281. The investment plan results in an annual $437,598 reduction in costs (9.06% saving per year). Line 80 connects bus 49 to bus 50 and the investment on this line at the first quarter allows NGU2 to inject free and more power to the network in whole year. Line 2 is also invested early in quarter 2 which connects bus 1 to bus 2. As the NGU1 is located at bus 1, expanding the transmission limit of line 2 allows NGU1 to commit more to the power generation at quarters 2, 3, and 4. Finally, the computation times for solving the decomposed version of the problem and for solving the compact version (Problem 5) are provided at Figure 16. The decomposition algorithm finds a good solution (with 1.5% optimality gap) in 2 hours

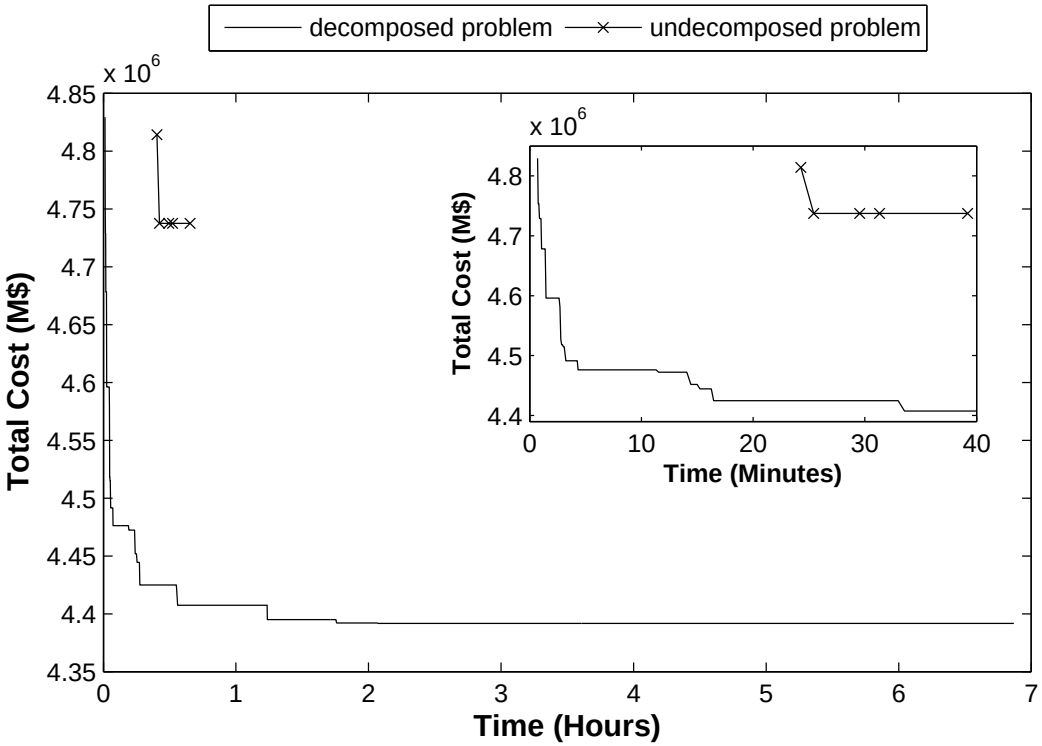


Figure 16: Computational Times (Study 3)

and reaches to 1% optimality gap in less than 7 hours. When the compact problem is solved, Gurobi finds a solution with the cost $4,737,500 after 25 minutes. The same solution is found by the decomposition algorithm after 53 seconds. The gurobi gets out of memory after 39 minutes of running time when it tries to solve the compact problem.

## 2.8 Conclusions

In this chapter a mathematical programming model was developed to facilitate the gradual integration of the dynamic ratings into electric transmission systems where the utilization of the dynamic ratings were also coordinated with the transmission switching operations. To solve the problem, we decomposed the model into a master problem and three subproblems. The master problem proposed potential optimal plans for the line investment and the line switching in each time period with the

goal of minimizing total investment and operation costs in the planning horizon. The subproblems evaluated the feasibility and optimality of the proposed plan in terms of the energy security and energy generation costs and reduced the search space of the master problem accordingly. We should emphasize that the developed decomposition algorithm in this chapter along with the tuning method for the disjunctive parameter can also be effectively used to solve the optimal transmission switching problem.

The solutions of our model found the optimal investment time and the best candidate lines to be invested. To study the effect of the dynamic rating uncertainty on the investment plan, we conducted a sensitivity analysis on the 118-bus system. We realized that the best candidate lines for the dynamic rating investment were not sensitive to volatilities in predicted ratings. Also as another favorable finding, the calculated investment plans included a low number of transmission lines compared to the total number of lines in the system. New transmission lines are expensive assets in terms of construction and installation, land usage, and environmental impact. The results of this chapter indicates the investments in the dynamic rating systems as an alternative to delay or possibly cancel the transmission expansion plans. More research is required to explore the relationships between our proposed dynamic rating expansion and the developed transmission expansion problems [12, 13, 26].

We also tested the utilization of two sample free generation units in presence of the dynamic ratings. The test results indicated that the dynamic ratings can play a key role in extending wind and solar farms and any other renewable sources of energy with free or low operational cost. We used the forecasted capacities for the thermal ratings and also for the test renewable sources in our long-term planning model. Developing short-term models for the daily operations is another research problem and requires further studies. Stochastic programing and optimization is one

possible modeling and solution method to deal with the uncertainties inherent in different sources of energy especially in renewable resources.

References

[1] P.M. Callahan and D.A. Douglass. An experimental evaluation of a thermal line uprating by conductor temperature and weather monitoring. *Power Delivery, IEEE Transactions on*, 3(4):1960–1967, 1988.

[2] Murray W. Davis. A new thermal rating approach: The real time thermal rating system for strategic overhead conductor transmission lines – part i: General description and justification of the real time thermal rating system. *Power Apparatus and Systems, IEEE Transactions on*, 96(3):803–809, 1977.

[3] H.E. House and P. D. Tuttle. Current-carrying capacity of ACSR. *Power apparatus and systems, part iii. transactions of the american institute of electrical engineers*, 77(3):1169–1173, 1958.

[4] Transmission conductors thermal ratings. *Paper 68-TAP-29, Report by Transmission Advisory Panel, East Central Area Reliability Coordination Agreement*, 1968.

[5] IEEE standard for calculating the current-Temperature of bare overhead conductors. *IEEE Std 738-2006 (Revision of IEEE Std 738-1993)*, pages c1–59, 2007.

[6] IEC Standard TR 1597. Overhead Electrical Conductors - Calculation Methods for Stranded Bare Conductors (1985).

[7] CIGRE Working Group 22.12. the thermal behaviour of overhead line conductors? *Electra*, vol. 114, no. 3:pp. 107125, 1992.

[8] O.A. Ciniglio and A.K. Deb. Optimizing transmission path utilization in idaho power. *Power Delivery, IEEE Transactions on*, 19(2):830–834, 2004.

[9] E.B. Fisher, R.P. O'Neill, and M.C. Ferris. Optimal transmission switching. *Power Systems, IEEE Transactions on*, 23(3):1346 –1355, aug. 2008.

[10] K.W. Hedman, R.P. O'Neill, E.B. Fisher, and S.S. Oren. Optimal transmission switching with contingency analysis. *Power Systems, IEEE Transactions on*, 24(3):1577 –1586, aug. 2009.

[11] K.W. Hedman, M.C. Ferris, R.P. O'Neill, E.B. Fisher, and S.S. Oren. Co-optimization of generation unit commitment and transmission switching with n-1 reliability. *Power Systems, IEEE Transactions on*, 25(2):1052 –1063, may 2010.

[12] J.C. Villumsen and A.B. Philpott. Investment in electricity networks with transmission switching. *European Journal of Operational Research*, 222(2):377 – 385, 2012.

[13] A. Khodaei, M. Shahidehpour, and S. Kamalinia. Transmission switching in expansion planning. *Power Systems, IEEE Transactions on*, 25(3):1722 –1733, aug. 2010.

[14] M. Jabarnejad, J. Wang, and J. Valenzuela. A decomposition approach for solving seasonal transmission switching. *Power Systems, IEEE Transactions on*, 30(3):1203–1211, May 2015.

[15] NERC Reliability Concepts. 2007.

[16] Dynamic Circuit Thermal Line Rating, Strategic Energy Research, California Energy Commission. October 1999.

[17] Stuart Malkin and Eric Hsieh. Beyond real time: the computational challenges of forecasting dynamic line ratings. *FERC Software Tech Conference*, June 26, 2013.

[18] S. Binato, M. V F Pereira, and S. Granville. A new benders decomposition approach to solve power transmission network design problems. *Power Systems, IEEE Transactions on*, 16(2):235–240, May 2001.

[19] J.F. Benders. Partitioning procedures for solving mixed-variables programming problems. *Numerische Mathematik*, 4(1):238–252, 1962.

[20] Riku Pasonen Sanna Uski-Joutsenvuo. Maximising power line transmission capability by employing dynamic line ratings. *technical survey and applicability in Finland*, 2013.

[21] ONCOR West Texas Dynamic Line Rating (DLR) Project, ERCOT RPG Overview. March 26, 2013.

[22] PJM Hourly Load Data.

[23] L.L. Garver. Transmission network estimation using linear programming. *Power Apparatus and Systems, IEEE Transactions on*, PAS-89(7):1688–1697, 1970.

[24] Power Systems Test Case Archive.

[25] C. Barrows and S. Blumsack. Transmission switching in the rts-96 test system. *Power Systems, IEEE Transactions on*, 27(2):1134 –1135, may 2012.

[26] C. Ruiz and A.J. Conejo. Robust transmission expansion planning. *European Journal of Operational Research*, (0):–, 2014.

# Chapter 3

## Emissions Reduction Using The Dynamic Line Switching and Rating

### 3.1 Abstract

Global warming and climate change are gradually affecting our planet and have now been considered as serious global issues that should be addressed in following years. The contributors to the gradual warming of our planet are the increasing concentrations of greenhouse gases and other human activities. The carbon dioxide ($CO_2$) is the major greenhouse gas. Every year, the electricity generation industry releases significant amount of carbon dioxide to the atmosphere by burning traditional sources of energy including coal and gas. Significant efforts have been made by the U.S. government and major electricity generation companies to reduce the usage of traditional and environmentally-unfriendly sources of energy and, in return, increase the level of electricity generation by the renewable and green sources of energy. To be able to increase the usage of renewable sources of energy and reduce the carbon-dioxide emissions in the electricity production, a dynamic electricity transmission network is also required. In this chapter, we extend our optimization model, developed in previous chapter, by including the element of emission reduction in addition to minimizing the electricity generation cost. We also investigate the effects of dynamic rating and transmission switching in the carbon-dioxide emission reduction, especially when the sources of energy are diverse.

**keywords:** electric power generation, emission reduction, transmission network, dynamic thermal rating, transmission switching, mixed integer linear programming.

### Notations

Indices

*Including the ones in Chapter 2.*

Sets

*Including the ones in Chapter 2.*

Parameters

$Q_n^{\mathrm{e}}$ Emission coefficient of generator $n$.

$TE$ Total emission allowed to be released.

*Including the ones in Chapter 2.*

Variables

*Including the ones in Chapter 2.*

## 3.2 Introduction

Global warming and climate change are gradually and adversely affecting our planet. The main reasons that cause the global warming are the increasing concentrations of greenhouse gases and other human activities [1, 2]. The carbon dioxide ($CO_2$) is the major greenhouse gas (82.5% of all green house gases [3]). On the timescale of centuries to a millennium, the extent of global warming will be assessed primarily by anthropogenic $CO_2$ emissions [4]. The reason for this is the very long lifetime of the carbon dioxide in the atmosphere. Therefore, balancing global average temperature would necessitate significant decreases in anthropogenic $CO_2$ emissions [4]. Reductions in emissions of other green house gases including methane and nitrous oxide would also be required. Even in the case of significant reductions in the anthropogenic $CO_2$, global average temperatures would remain close to their highest level for many hundreds of years [4].

Every year, the electricity generation industry releases significant amount of $CO_2$ to the atmosphere. In 2012 in U.S., more than 2000 million metric tons of $CO_2$ equivlent emission was generated by the electricity generation industry (the highest

emission level among other sectors [3]). Burning coal and gas are main causes of $CO_2$ emissions in the electricity generation market. Currently, coal is the most used source of energy for the electricity generation. Around 39% of U.S. electricity is produced by burning coal. Natural gas and nuclear are the second and third most used energy source with 27% and 19% share, respectively. Approximately, 13% of U.S. electricity is generated using renewable resources [3]. Due to significant efforts made by the U.S. government and major electricity generation companies, the usage of traditional and environmentally-unfriendly sources of energy are reducing. For instance, the capacity of coal power plants in the U.S. is slightly shrinking. In return, the level of electricity generation by the renewable and green sources of energy are increasing. It is expected that by 2050, 80% of U.S. electricity be generated using renewable sources [5].

The renewable-energy increasing trend leads to future dependencies on both traditional and renewable sources of energy which are naturally disseminated in different geographies and are often far from major energy consumption centers. The geographical distributions for four types of renewable sources in the United States are depicted in Figure 17. In the U.S. map at the top-left of the Figure 17, it is shown that the east and west coasts along with central parts of the country enjoy a considerably (and on average) high wind speed throughout the year. In the U.S. map at the top-right, the distribution of the potential solar power capacity is depicted where the southwest of the country (e.g. New Mexico, Arizona, and Nevada) has very high solar capacity while the northeast has the least. The hydro power sources in the United States are shown in the bottom-left map which indicates the states in the northwest have the best potential. Finally, the map at the bottom-right depicts the geographical distribution of the biomass power plants in the country which indicates that majority of the biomass energy infrastructure are currently at southeast, northeast, and west coast. As the maps suggest, the renewable sources of energy are dispersed in different

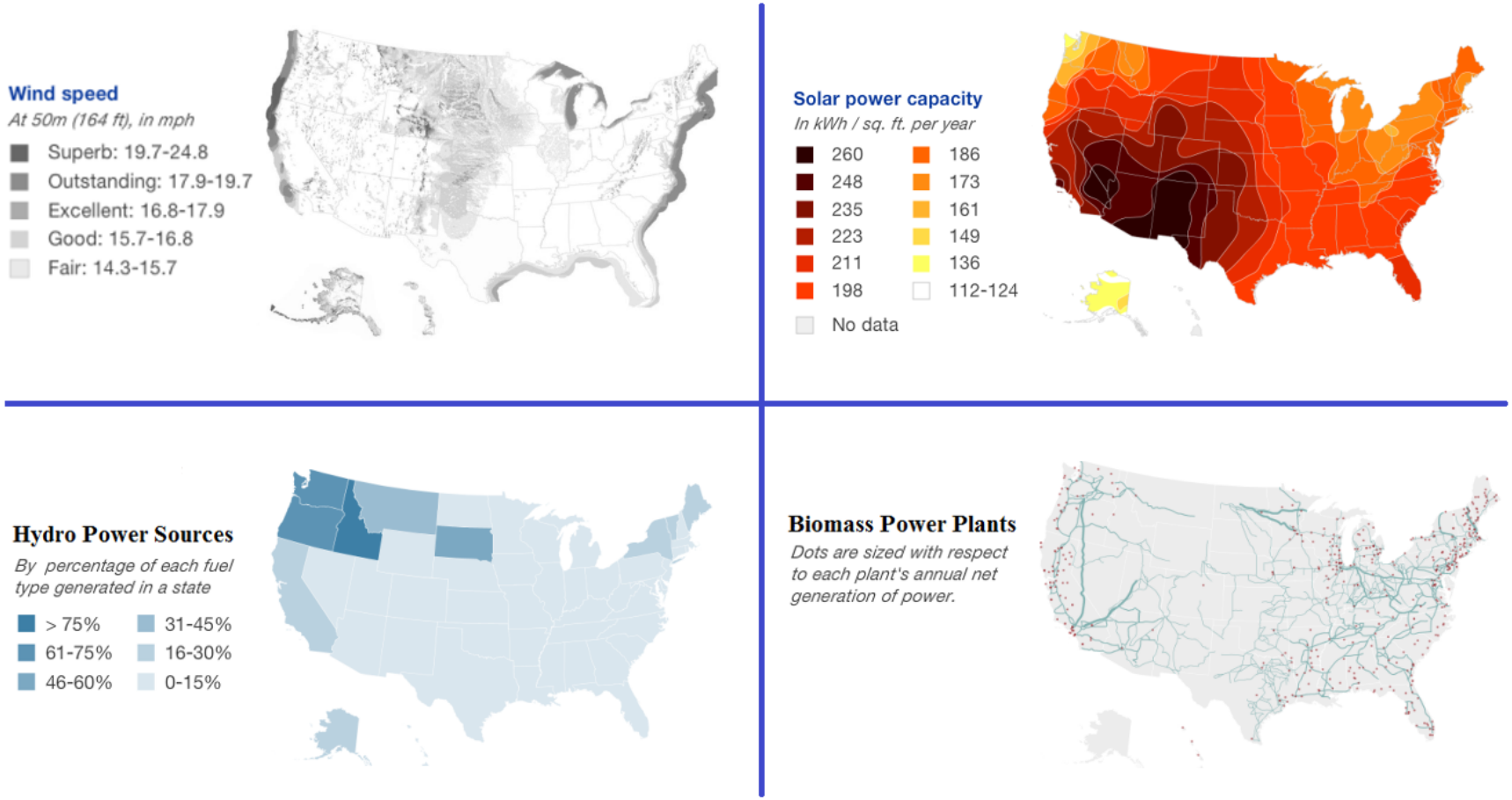


Figure 17: Geographical Distribution of Sustainable Energies [6]

corners of the country. How to efficiently transmit these diverse and disseminated sources of energy is one of the greatest management challenges in the future smart grids. To be able to increase the usage of diverse renewable sources of energy and reduce the carbon-dioxide emissions in the electricity production, a dynamic electricity transmission network is also required. The transmission management approaches, proposed in this dissertation, can lead to the emission reduction in the power systems and, therefore, to a better environmentally-friendly utilization of the energy sources. In the following sections, we extend our transmission management models to the case where the emission reduction is also respected in the electricity generation operations.

### 3.3 The Emission Reduction Model

Different approaches have been investigated for emission reduction in the economic power dispatch. In [7] a minimum emission power flow is developed in which the fuel cost and emissions are included in the objective function. Then the trade-off between fuel cost and emissions is investigated. A summary of already developed methods for environmental-economic dispatch in electric power systems is provided in [8]. According to [8], the reduction in air-pollutants is achieved by including emissions either as a constraint or as a weighted function in the objective of the overall dispatching problem. In [9] a scheme for the decisions on power systems operation is proposed based on fuzzy economic and environmental dispatch. A power transmission expansion plan considering the carbon dioxide emission is developed in [10] where the carbon-dioxide emission price is modeled as a probability density function in the transmission network planning problem. Also, a combined generation and transmission expansion model is introduced in [11] to avoid wasting of existing renewable generation sources. A multi-objective optimization algorithm is introduced in [12] for solving the combined economic emission dispatch problem with valve point loading.

In this chapter, we extend our optimization model, developed in previous chapter, by including the element of emission reduction in addition to minimizing the electricity generation cost. As minimizing the fuel cost and emission reduction are two conflicting objectives, simultaneously minimizing both objectives can be problematic. Our goal is to find the minimum electricity generation cost where the model is constrained to a certain maximum level of emission. Our combined economic emission dispatch problem is described by (15a) to (15c).

$$\min \quad \sum_{t}\sum_{k}\frac{C^{\mathrm{d}}_{k}\,x_{tk}}{(1+i)^{t-1}}+\sum_{t}\sum_{l}\sum_{n}\frac{H_l\,C^{\mathrm{g}}_{n}\,g_{tl0n}}{(1+i)^{t-1}} \tag{15a}$$

Subject to

$$\sum_{t}\sum_{l}\sum_{n}H_l\,Q^{\mathrm{e}}_{n}\,g_{tl0n}\leq TE \tag{15b}$$

$$\text{Constraints } (5b)\text{–}(5o) \tag{15c}$$

The objective function (15a) minimizes the total cost of investment on the DTR equipment and also the electricity generation cost where there is no contingency in the power system. As it was the case in problem (5), the electricity generation cost at all hours is calculated as the generation cost of the load blocks multiplied by their durations in terms of number of hours ($H$). The constraint (15b) ensures that the cumulative amount of emissions does not exceed the pre-specified upper-bound $TE$. The rest of constraints (i.e. the constraints (15c)) are the same with the ones in problem (5).

### 3.4 Numerical Experiments

In this section, we investigate the effects of dynamic rating and transmission switching in the carbon-dioxide emission reduction. The investment model (15) is studied

on both the Garver's system and the IEEE 118-bus system. A value of $\pm 1.2$ radians is considered for minimum/maximum phase angle differences. The installation, maintenance, and transmission switching costs are ignored. As the installation time for the DTR equipment is short [13], the outage time for lines under the equipment installation is not considered. The PJM hourly load data [14] for sub-zone PN for year 2011 is normalized by scaling between 0 and 1 and then the normalized data is multiplied by the system load to generate demand in different hours of the year. A load growth rate is used to estimate the future loads. To reduce the size of the problem, a year is divided to four quarters and each quarter is divided to three load blocks of low, average, and high. The profile of loads is provided in Table 7 in Chapter 2. The number of loads falling in each load block is considered as the duration of that load block and is used in the cost weight vector $H$. An unlimited budget for the capital dynamic rating investment is assumed. All recurring costs, including operational and investment, are assumed to be the same in future time periods.

### 3.5 Garver's System

The Garver's system in [15] is modified in this study in the same way explained in Section 2.6 (also illustrated in Figure 11 in Chapter 2). The data for the transmission lines is provided in Table 9 of Chapter 2. The loads and generation units are summarized in Table 16 where the data for the generation cost and emission level per energy source are obtained from [9, 16]. For the modified Garver's system, it is assumed that $E = 50/X$. Also an investment cost of \$50,000 is considered for every line. A 3-year planning horizon (12 quarters) is considered for the investment model. For each invested line, 130% of the static rating is utilized. In each quarter, up to 2 lines are allowed both for the DTR investment and for the switching. The results are summarized in Table 17.

Table 16: Load and generation data for Garver's system

| Bus No. | Load (MW) | Energy Source | Generating Capacity (MW) | Cost Rate ($/MW·h) | Emission Rate (kg/MW·h) |
|---|---|---|---|---|---|
| 1 | 32 | Oil, 1.3% s | 150 | 26.08 | 713.21 |
| 2 | 96 | – | – | – | – |
| 3 | 16 | Gas | 360 | 22.31 | 414.16 |
| 4 | 64 | – | – | – | – |
| 5 | 96 | – | – | – | – |
| 6 | – | Coal, 1.83% s | 600 | 14.96 | 959.99 |

If there is no restriction on the emission level (i.e. if $TE = +\infty$) and when there is no investment on the DTR technology and no TS is practiced, totally 4,624,000 tons of $CO_2$ is released to the atmosphere during the three-year operation. If the DTR and TS are considered with no restriction on the emission level, then the emission amount increases to 4,996,100 tons of $CO_2$. This is because the model finds the cheapest solution in terms of the electricity generation cost (5.55% cheaper than the case with no DTR and no switching) when no restriction on the emissions is applied. However, as shown in the Table 17, when the emission is constrained to the certain maximum values, utilizing the DTR and TS meets the carbon-dioxide release restrictions and, at the same time, a cheaper solution is achieved. The highest reduction in the generation cost (1.75%) is achieved in the case of 2.5M ton-$co_2$ maximum emission in 3 years. Another interesting result is that with the 2.4M ton-$co_2$ maximum emission in 3-year constraint, the system cannot meet the electricity demand if the DTR and TS are not utilized. The system with the DTR and TS utilization still cannot operate with the 3-year maximum emission restriction of 2M ton-$co_2$ or lower.

Table 17: Emission Reduction in Garver's system with Coal Power Plant

| | No DTR No SW | DTR + TS | |
|---|---|---|---|
| Max Emission (ton-$co_2$) | Generation Cost ($) | Generation Cost ($) | Reduction in Cost |
| – | 78,528,593 | 74,172,556 | 5.55% |
| 4,500,000 | 79,871,016 | 79,588,206 | 0.35% |
| 4,000,000 | 85,473,219 | 85,351,783 | 0.14% |
| 3,500,000 | 91,425,033 | 91,399,214 | 0.03% |
| 3,000,000 | 97,746,846 | 97,725,780 | 0.02% |
| 2,500,000 | 106,562,879 | 104,700,565 | 1.75% |
| 2,400,000 | INF | 106,511,207 | N/A |
| 2,000,000 | INF | INF | N/A |

As mentioned in the introduction section, the capacity of coal power plants in the U.S. is slightly shrinking and their capacity expected to be gradually replaced by the renewable sources. To see how much the DTR and TS can save emissions in the future, we replace the coal power plant at bus 6 in the Garver's system (See Table 16) with a wind farm and run the model again. The wind farm capacity is assumed to be the same (600 MW) but with \$0/MW·h cost rate and with 21kg/MW·h emission rate. If there is no restriction on the emission level, there is no investment on the DTR technology, and no TS is practiced, then totally 492,390 tons of $CO_2$ is released to the atmosphere during the three-year operation with the replaced wind farm. With the DTR and TS and with no restriction on the emission level, surprisingly the emission amount decreases to 224,320 tons of $CO_2$. This is more than one-half (54.44%) reduction in the emissions. The total electricity generation cost in 3 years without the DTR and TS is \$19,367,388. The same cost drops to \$5,841,877 when both the

DTR and TS are employed. Using the DTR and TS results in a significant reduction of 69.84% in costs as well. When the emission is constrained to values lower than 224,320 tons of $CO_2$ in 3 years, the power system cannot meet the carbon-dioxide release restrictions, whether the DTR and TS are utilized or not. We conclude that the 224,320 tons of $CO_2$ in 3 years is the minimum emission level achieved by the model. The reason for this is that the capacity of the wind farm is fully employed during different quarters. As the wind farm has the lowest carbon-dioxide consequences in this typical system, further improving the emission levels in this power system with current generation profile is impossible. The 54.44% reduction in the emissions of this Garver's system is achieved by investing on the DTR technology at lines 2–6 and 4–6 and by switching one or two of lines 1–2, 2–3, or 2–4 in different quarters.

### 3.6 IEEE 118-bus System

Data for the IEEE 118-bus power system is downloaded from [17] where generators' capacity, generation costs, transmission network and line characteristics are taken from [18]. The system is the same with the one summarized in Table 12 in Section 2.7. As the focus of this section is to investigate the emission reduction, the single contingency scenarios are relaxed in this section on the 118-bus system to obtain the results in shorter time. The generation costs for the 118-bus system are on the order of 50 to 100 times smaller than typical generator costs. We use these costs to be consistent with the results and developed models published in the literature. Therefore, for this power system we consider a lower DTR investment cost of \$1000 for every line. We assume a planning horizon of one year (4 quarters) and an annual discounting rate of 10%, compounded quarterly. The 110% of the average load blocks in Table 7 in Section 2.7 are used as the quarterly demand profiles with durations 2160, 2184, 2208, and 2208 for 1st, 2d, 3rd, and 4th quarters, respectively. For each invested line, 130% of the static ratings are utilized. At most, two lines per quarter

are considered for the DTR investment and two lines per quarter for the switching. The following three scenarios are considered.

- Scenario 1: It is assumed that all 19 thermal generators use coal to generate power.
- Scenario 2: It is assumed that generators at buses 10, 12, 25, 26, 31, 46 use oil, generators at buses 49, 54, 59, 61, 65, 66 use gas, and generators at buses 69, 80, 87, 92, 100, 103, 111 use coal to generate power.
- Scenario 3: It is assumed that all 19 thermal generators are coal power plants plus two additional wind farms. One wind farm is considered for bus 1 and another one for bus 50. The capacity of each wind farm is assumed to be 450MW.

In above scenarios, the same cost and emission rates shown in Table 16 are used for the oil, gas, and coal. In addition, each wind farm is assumed to have \$0/MW·h cost rate and 21kg/MW·h emission rate. In Scenario 1, if there is no restriction on the emission level (i.e. if $TE = +\infty$) and when there is no investment on the DTR technology and no TS is practiced, totally 27,577,000 tons of $CO_2$ is released to the atmosphere in one year of operations. If the DTR and TS are considered with no restriction on the emission level, then the emission amount is the same. This is because, there is no diversity in the energy sources as all generation units are assumed to be coal power plants. However, the model finds a cheaper solution of \$6,356,272 per year in terms of the electricity generation cost (1.55% cheaper) when the DTR and TS are used. When the emission is constrained to 27,400,000 tons of $CO_2$ or lower, the system gets infeasible even when the DTR and TS are practiced.

Things change when we move to Scenarios 2 in which we include diverse sources of energy in the 118-bus power system. In Scenario 2, if there is no restriction on

Table 18: Emission Reduction in 118-bus system with Oil, Gas, and Coal Plants (Scenario 2)

| | No DTR No SW | DTR + TS | |
|---|---|---|---|
| Max Emission (ton-$co_2$) | Generation Cost ($) | Generation Cost ($) | Reduction in Cost |
| – | 6,456,241 | 6,355,446 | 1.56% |
| 20,500,000 | 6,858,443 | 6,550,243 | 4.49% |
| 20,000,000 | 7,131,185 | 6,792,512 | 4.75% |
| 19,500,000 | 7,864,228 | 7,037,819 | 10.51% |
| 19,000,000 | 15,597,357 | 7,353,197 | 52.86% |
| 18,500,000 | INF | 7,715,364 | N/A |
| 18,000,000 | INF | 8,131,247 | N/A |
| 16,800,000 | INF | INF | N/A |

the emission level and with investing on the DTR and with practicing TS, the total electricity generation cost to supply the demand over one year is $6,355,446. This comes with an emission level of 21,009,000 tons of $CO_2$ per year. If no investment is made on the dynamic rating and no transmission switching is practiced, then total cost increases to $6,456,241 and total emission level increases to 21,373,000 tons of $CO_2$. The investment plan results in 1.56% reduction in annual costs and 1.70% reduction in annual carbon-dioxide emission. Further results are summarized in Table 18.

In all experiments summarized in Table 18, utilizing the DTR and TS meets the carbon-dioxide release restrictions and, at the same time, a cheaper solution is achieved. The best reduction in the generation cost (52.86%) is achieved in the case of 19M ton-$co_2$ maximum emission in 1 year. Another interesting result is that with 18.9M ton-$co_2$ annual maximum emission, the system cannot meet the electricity

demand if the DTR and TS are not utilized. The system cannot operate with annual maximum emission restriction of 16.8M ton-$co_2$ or lower even if the DTR and TS are utilized. This means that utilizing the DTR and TS can further reduce the carbon-dioxide emissions for more than 11% (from 18.9M ton-$co_2$ to 16.8M ton-$co_2$) while it is not possible to do if no DTR and no TS policy is proceeded.

Finally, we conduct the experiments under Scenario 3 when two wind farms are added to the power system. With no restriction on the emission level, no investment on the DTR technology, and no TS practice, totally 21,237,000 tons of $CO_2$ is released to the atmosphere in one year of operations. Also, the annual electricity generation cost is \$4,823,379. If the DTR and TS are considered with no restriction on the emission level, then the emission amount is reduced to 20,195,000 (4.91% reduction). In addition, the model finds a much cheaper solution of \$4,329,567 per year in terms of the electricity generation cost. This is \$493,812 (almost half million dollar) saving per year (or 10.24% reduction in costs) when the DTR and TS are used. When the emission is constrained to 20M tons of $CO_2$ or lower, the system gets infeasible even when the DTR and TS are practiced.

## 3.7 Conclusions

The carbon dioxide ($CO_2$) is currently the major greenhouse gas and every year the electricity generation industry releases significant amount of this gas to the atmosphere. To be able to increase the usage of renewable sources of energy and reduce the carbon-dioxide emissions in the electricity production, a dynamic electricity transmission network is required. In this chapter, we extended our optimization model by including the element of emission reduction in addition to minimizing the electricity generation cost. Then we investigated the effects of dynamic rating and transmission switching in the carbon-dioxide emission reduction. In the experiments on both the

Garver's system and the IEEE 118-bus system, the proposed transmission management system reduced the emission levels significantly. Furthermore, our approach was able to supply the demand for the electricity with lower cost. Our approach could reduce the costs and emissions the best whenever the sources of energy were diverse in nature and they were scattered in different buses of the power systems.

References

[1] America's Climate Choices: Panel on Advancing the Science of Climate Change; National Research Council. *Advancing the Science of Climate Change*. 2010.

[2] CLIMATE CHANGE 2014: Synthesis Report. Summary for Policymakers. IPCC. Retrieved 7 March 2015.

[3] United States Environmental Protection Agency.

[4] National Research Council. *Climate Stabilization Targets: Emissions, Concentrations, and Impacts over Decades to Millennia*. 2011.

[5] Department of Energy's National Renewable Energy Laboratory (NREL).

[6] American Electric Power, American Wind Energy Association, Center for American Progress, Department of Energy, Edison Electric Institute, Energy Information Administration, Electric Power Research Institute, Federal Energy Regulatory Commission, National Renewable Energy Laboratory, U.S. Environmental Protection Agency, Western Resource Advocates, National Public Radio.

[7] J.H. Talaq, F. El-Hawary, and M.E. El-Hawary. Minimum emissions power flow. *Power Systems, IEEE Transactions on*, 9(1):429–435, Feb 1994.

[8] J.H. Talaq, F. El-Hawary, and M.E. El-Hawary. A summary of environmental/economic dispatch algorithms. *Power Systems, IEEE Transactions on*, 9(3):1508–1516, Aug 1994.

[9] M.F. Bedrinana, J.A. Bosco, C.A.F. Murari, and C.A. Castro. Decisions in power system operation based on fuzzy economic and environmental dispatch. In *Power Tech, 2007 IEEE Lausanne*, pages 1296–1301, July 2007.

[10] A.K. Kazerooni and J. Mutale. Transmission network planning under security and environmental constraints. *Power Systems, IEEE Transactions on*, 25(2):1169–1178, May 2010.

[11] R. Bent and G.L. Toole. Grid expansion planning for carbon emissions reduction. In *Power and Energy Society General Meeting, 2012 IEEE*, pages 1–8, July 2012.

[12] M. Rajkumar, K. Mahadevan, S. Kannan, and S. Baskar. Combined economic and emission dispatch with valve-point loading of thermal generators using modified NSGA-II. *JOURNAL OF ELECTRICAL ENGINEERING & TECHNOLOGY*, 8(3):490–498, 2013.

[13] ONCOR West Texas Dynamic Line Rating (DLR) Project, ERCOT RPG Overview. March 26, 2013.

[14] PJM Hourly Load Data.

[15] L.L. Garver. Transmission network estimation using linear programming. *Power Apparatus and Systems, IEEE Transactions on*, PAS-89(7):1688–1697, 1970.

[16] T. Gjengedal, S. Johansen, and O. Hansen. A qualitative approach to economic-environment dispatch-treatment of multiple pollutants. *Energy Conversion, IEEE Transactions on*, 7(3):367–373, Sep 1992.

[17] Power Systems Test Case Archive.

[18] E.B. Fisher, R.P. O'Neill, and M.C. Ferris. Optimal transmission switching. *Power Systems, IEEE Transactions on*, 23(3):1346 –1355, aug. 2008.